Structural and magnetic properties of superconductor / Yttrium Iron Garnet heterostructures with Bi and Nb

Mario Amado, L. McKenzie-Sell, A. di Bernardo, J. Robinson

Device Materials Group, University of Cambridge

C. Ciccarelli, Optoelectronics Cambridge

S. Ruiz, L. Perez *et al.* UCM Madrid

MARIE CURIE ACTIONS

The Leverhulme Trust

THE WINTON PROGRAMME FOR THE Physics of Sustainability MATERIALS DISCOVERY

THE ROYAL SOCIETY

EPSRC Engineering and Physical Sciences Research Council

Outline

1. Motivation
2. Growth and characterization of bare YIG thin films
3. Nb/YIG
4. Bi/YIG and BiCu/YIG

Spintronics

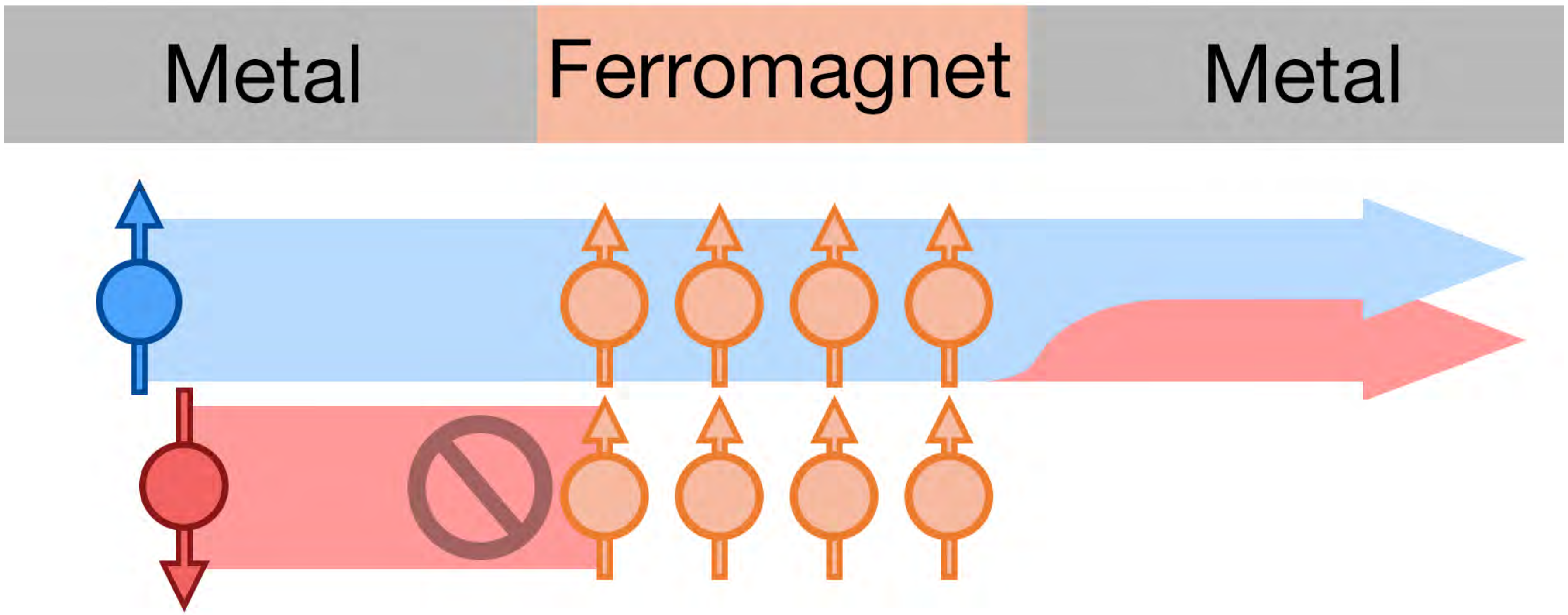

Superconducting spintronics

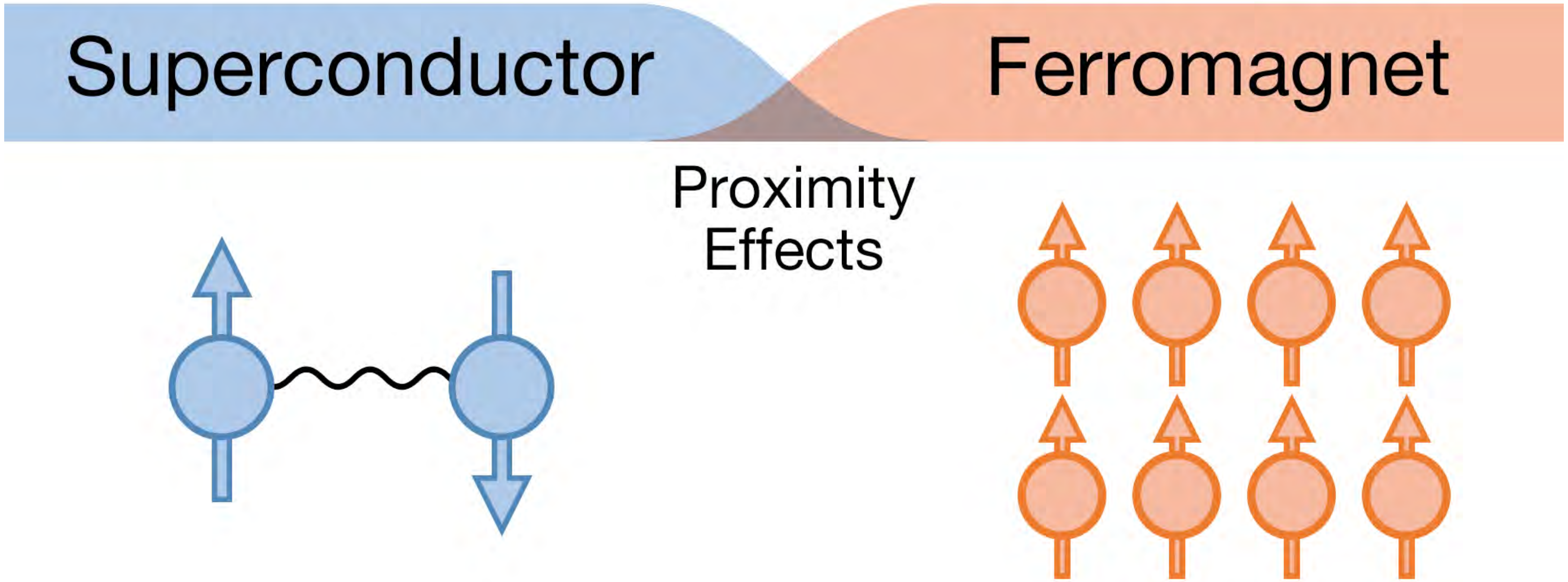

Superconducting DOS, Zeeman split S

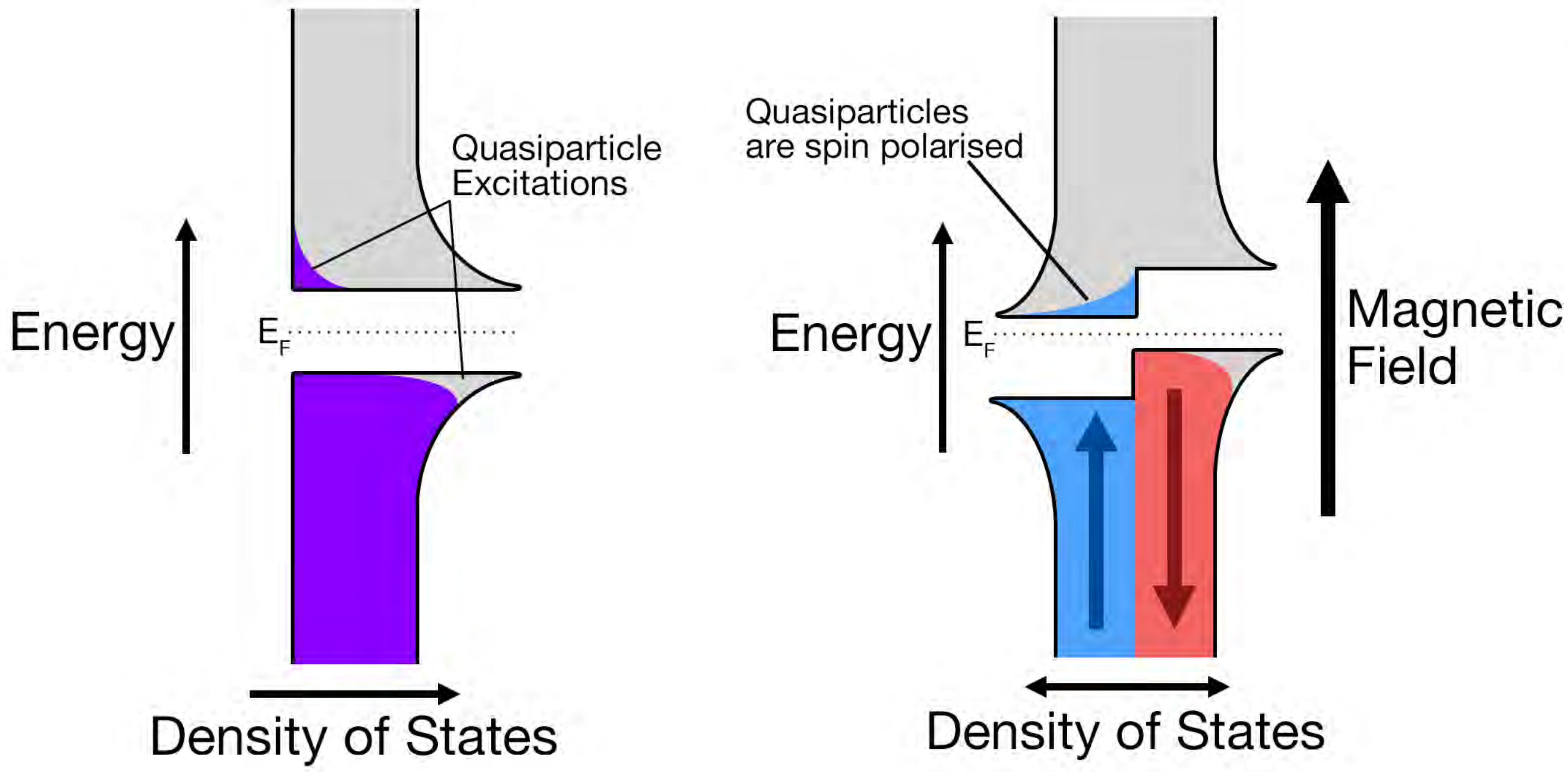

Yttrium Iron Garnet (YIG) properties

Yttrium Iron Garnet (YIG) properties

- YIG ($Y_3Fe_5O_{12}$)
  - Cubic unit cell: 160 atoms
  - Y^{3+} ions (black) coordinated by eight O^{2-} ions (red)
  - Fe^{3+} ions (white): 2 octahedral, 3 tetrahedral sites

Resistivity $\rho > 10^{12}$ Ωm

Curie temperature 550 K

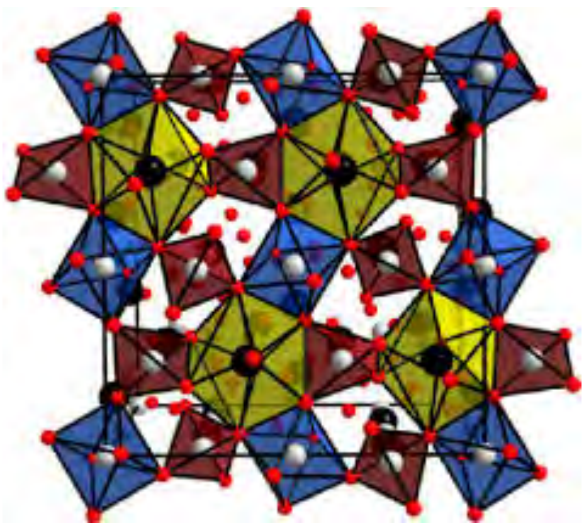

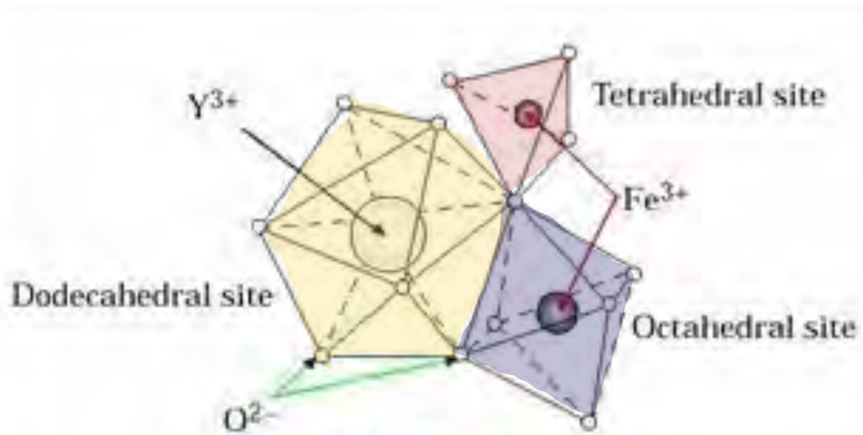

Yttrium Iron Garnet (YIG) properties

- **Ferrimagnetic**
  - Iron ion coordination sites exhibit different spins
  - $Y_3Fe_2Fe_3O_{12}$

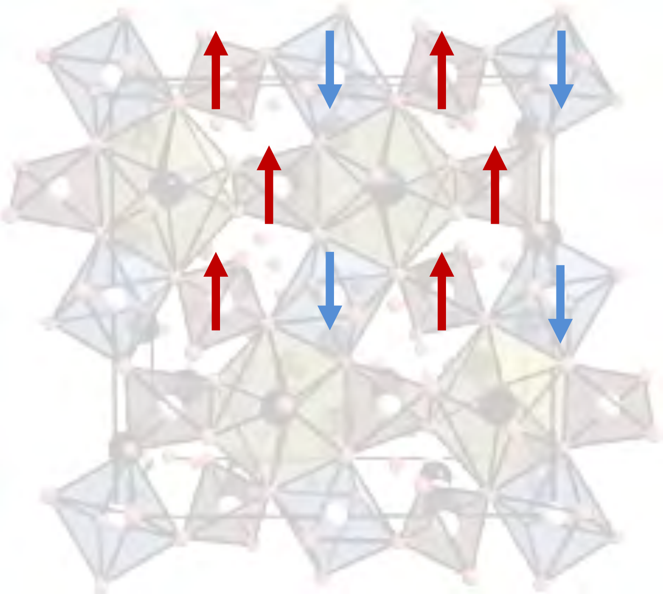

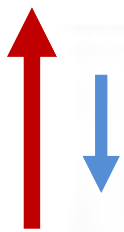

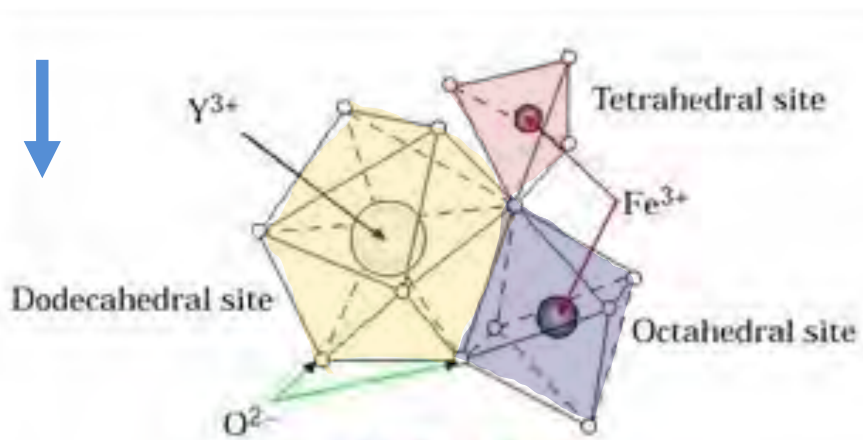

Why thin YIG?

YIG grown by liquid phase epitaxy (LPE) is high quality, but usually > 2 um thick

This is good for exciting spin wave modes…
… but not as effective for spin pumping, for which the uniform mode dominates

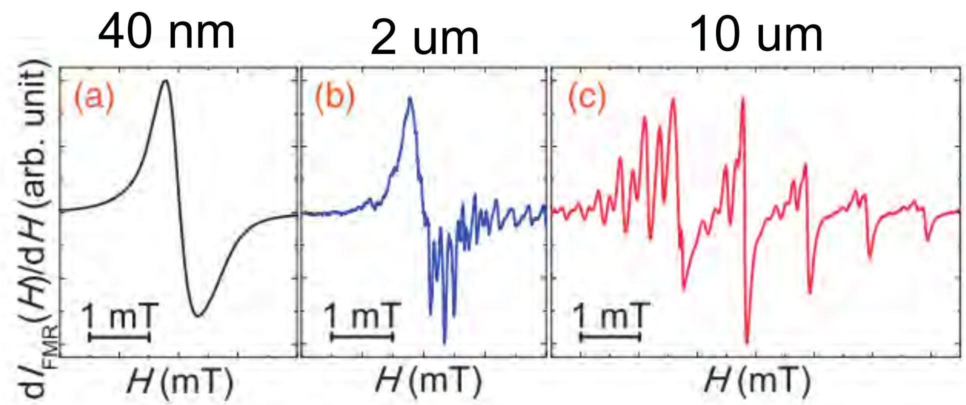

Fig. 1. Derivative absorbance FMR spectra of (a) $d_{YIG} = 40$ nm, (b) $d_{YIG} = 2$ µm, and (c) $d_{YIG} = 10$ µm YIG layers at $T = 297$ K for the in-plane static external magnetic field configuration.

Dushenko, S., Higuchi, Y., Ando, Y., Shinjo, T., & Shiraishi, M. (2015). Ferromagnetic resonance and spin pumping efficiency for inverse spin-Hall effect normalization in yttrium-iron-garnet-based systems. *Applied Physics Express*, *8*(10), 103002. https://doi.org/10.7567/APEX.8.103002

YIG: Growth and characterization

Growth methods: VPE, Hydrothermal growth, LPE DC/RF-Sputtering

- Pulsed laser deposition
  - < 100 nm thick
  - $Gd_3Ga_5O_{12}$ (GGG)
  - High temperatures (>750°C)
  - Low O_2 pressure

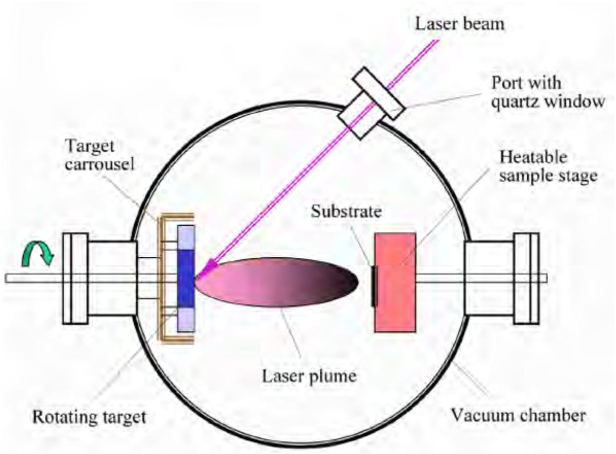

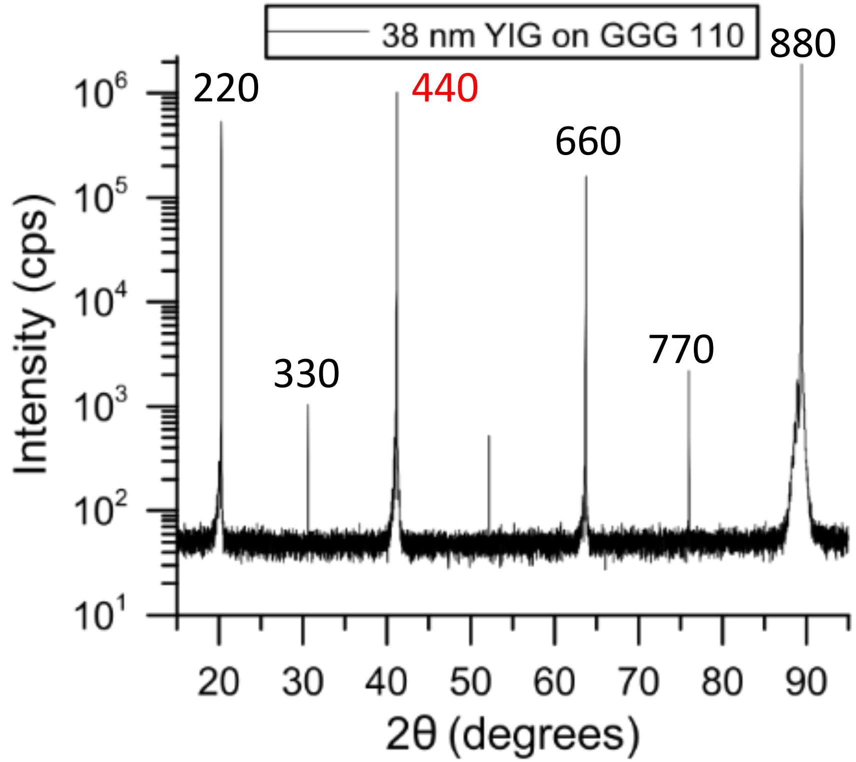

YIG: Growth and characterization

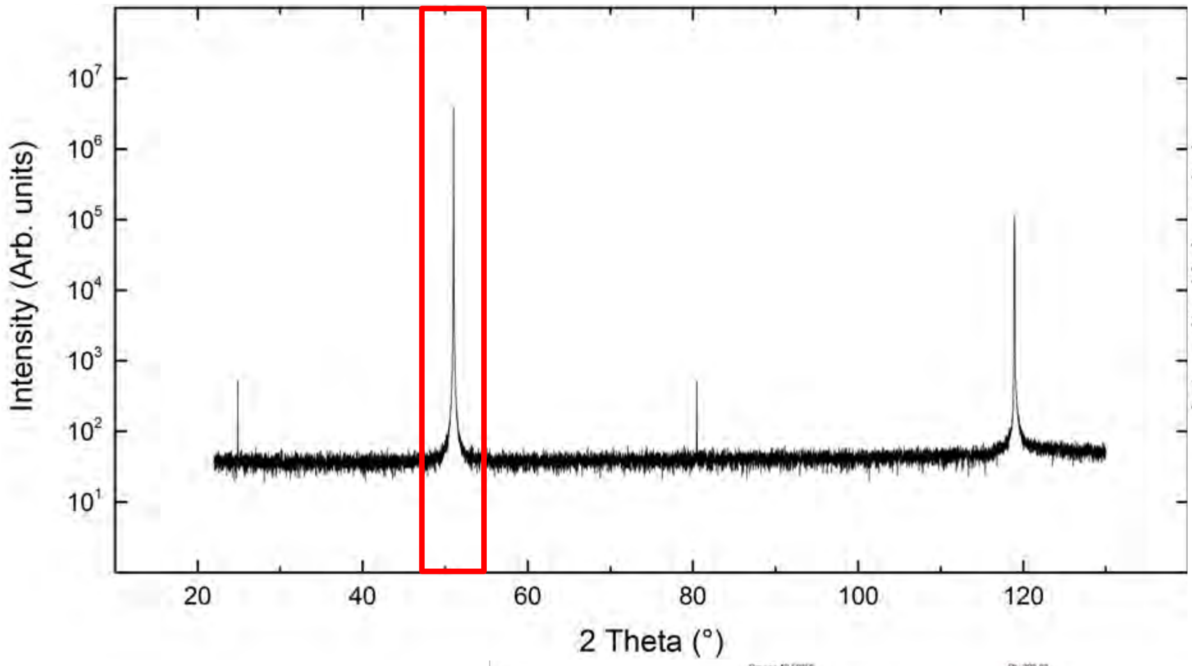

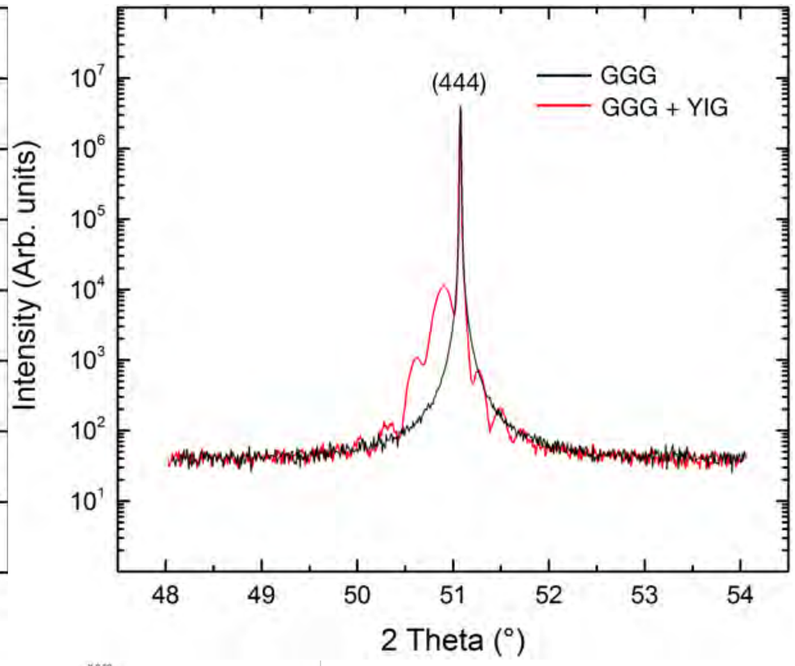

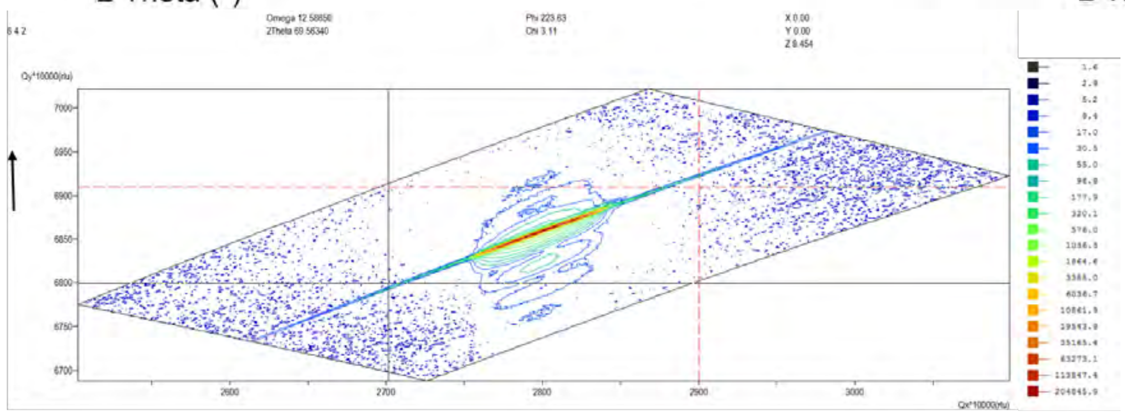

In-plane →

YIG: Growth and characterization

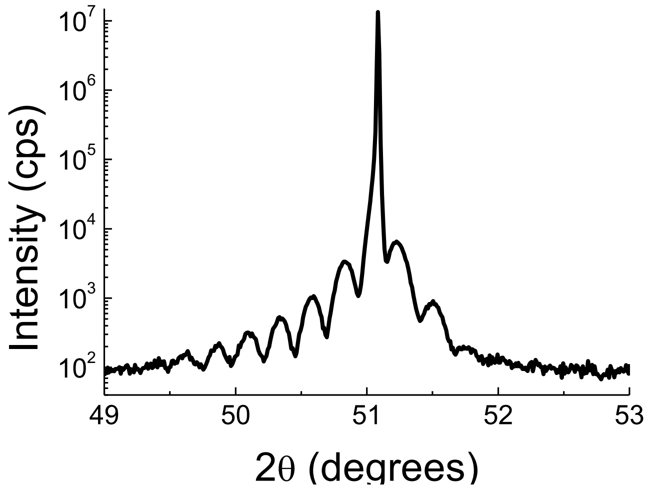

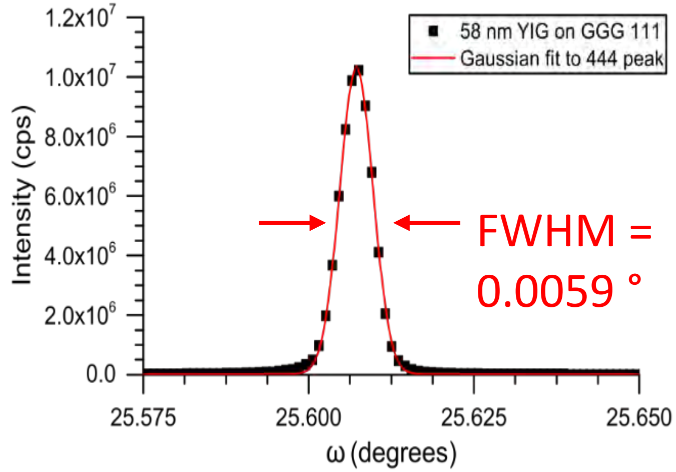

Better than 0.015 ° from Hauser Scientific Reports (2016)

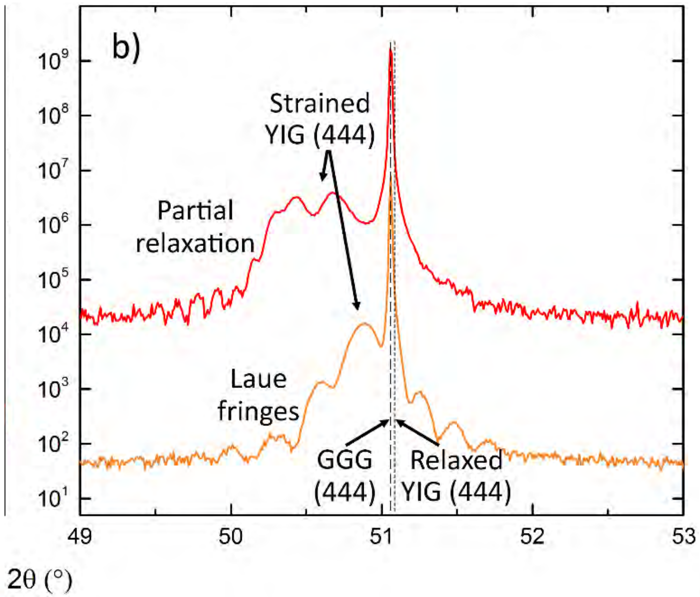

YIG	12.376 ± 0.004 Å [1]
GGG	12.383 Å [2]

Here YIG has extended out-of-plane lattice parameter

[1] Wang, X. *Metallic Spintronic Devices*. (2014).
[2] Tang, C. *et al. Phys. Rev. B* **94,** 1–5 (2016).

YIG: Growth and characterization

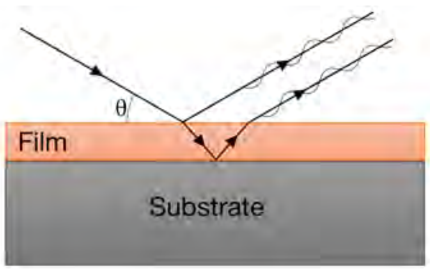

82 nm thick film

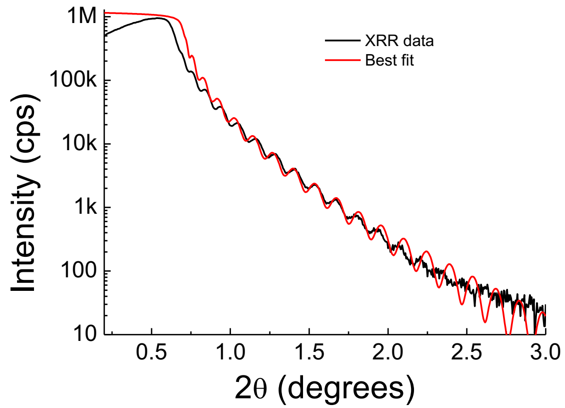

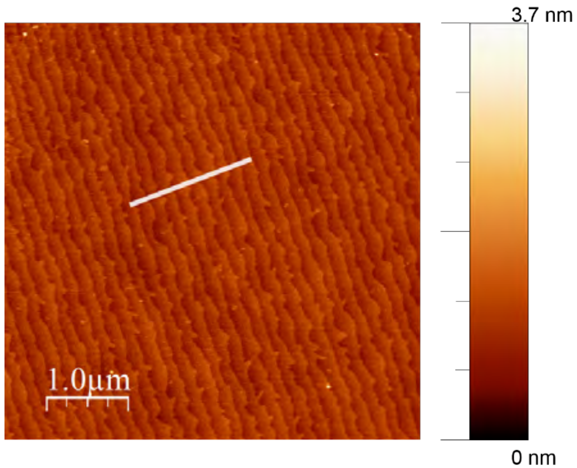

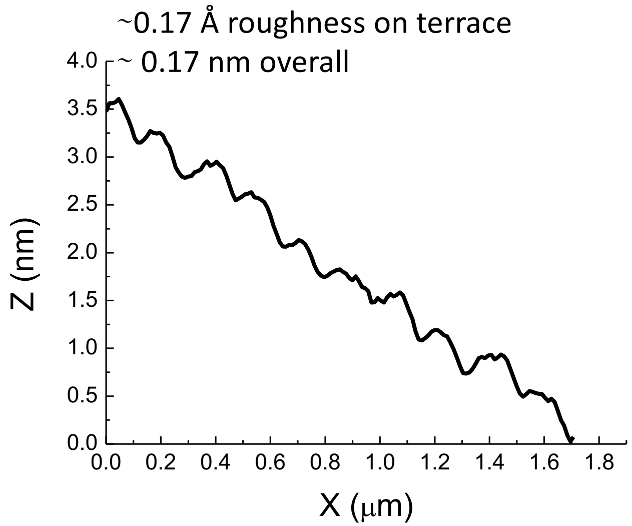

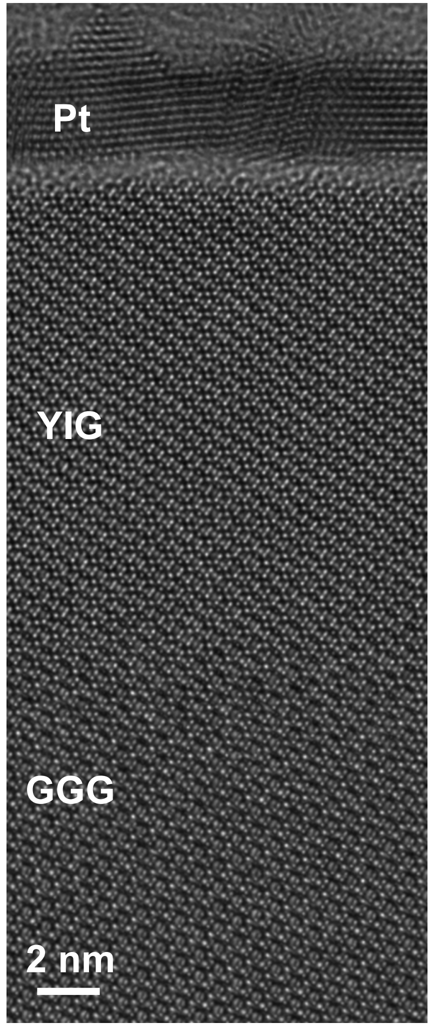

Courtesy of S. Velez, J. Gomez, F. Casanova and L. Hueso @ Nanogune

YIG magnetic anisotropy - VSM

Courtesy of
Graham Kimbell

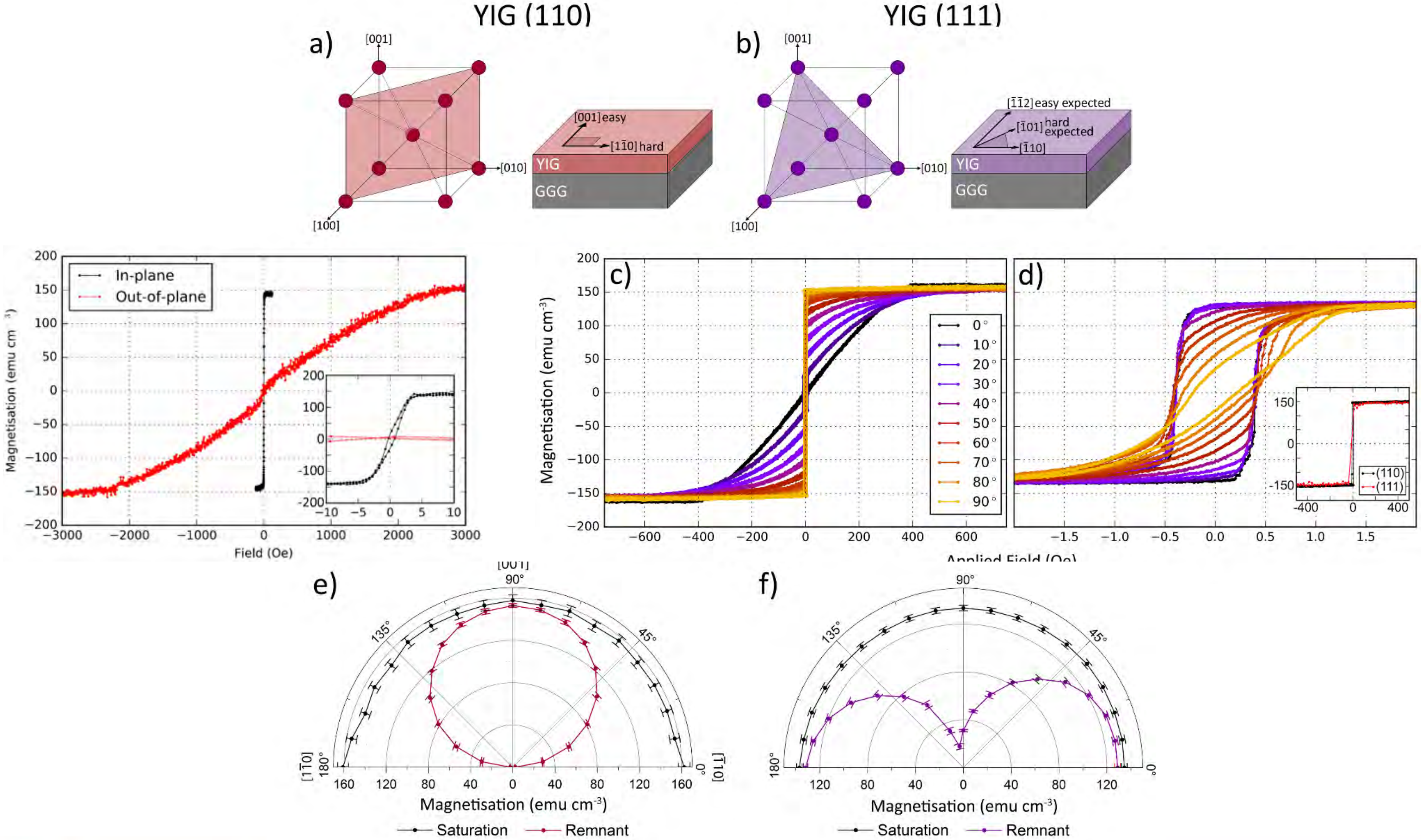

Experiments involving YIG

nature physics LETTERS
PUBLISHED ONLINE: 14 SEPTEMBER 2015 | DOI: 10.1038/NPHYS3465

Long-distance transport of magnon spin information in a magnetic insulator at room temperature

L. J. Cornelissen[1*], J. Liu[1], R. A. Duine[2], J. Ben Youssef[3] and B. J. van Wees[1]

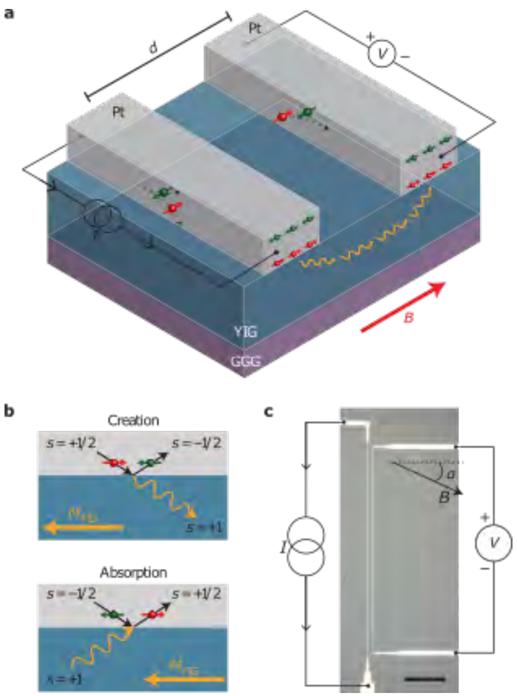

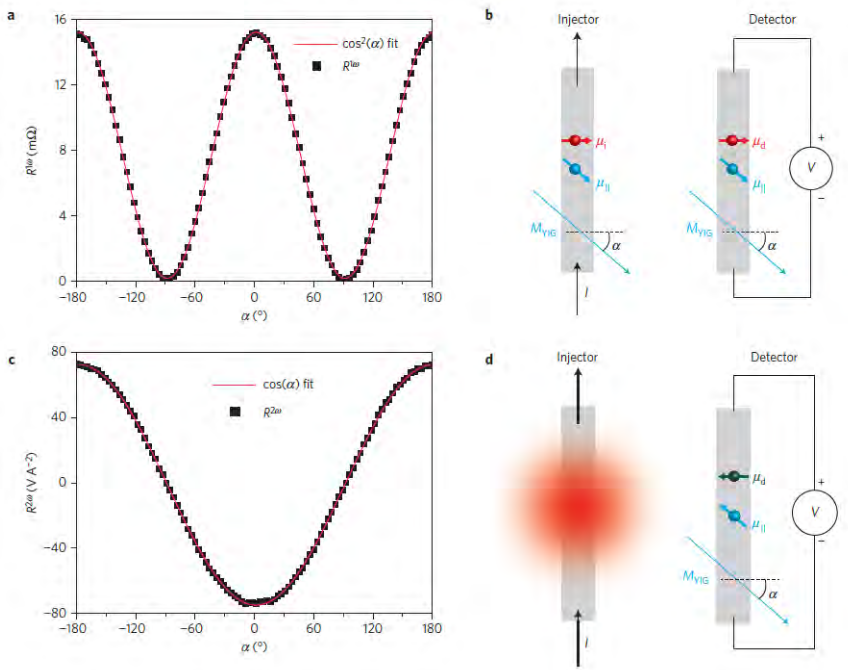

RAPID COMMUNICATIONS

PHYSICAL REVIEW B **93**, 020403(R) (2016)

Magnetic field dependence of the magnon spin diffusion length in the magnetic insulator yttrium iron garnet

L. J. Cornelissen* and B. J. van Wees

Physics of Nanodevices, Zernike Institute for Advanced Materials, University of Groningen, Nijenborgh 4, 9747 AG Groningen, The Netherlands

(Received 4 December 2015; published 19 January 2016)

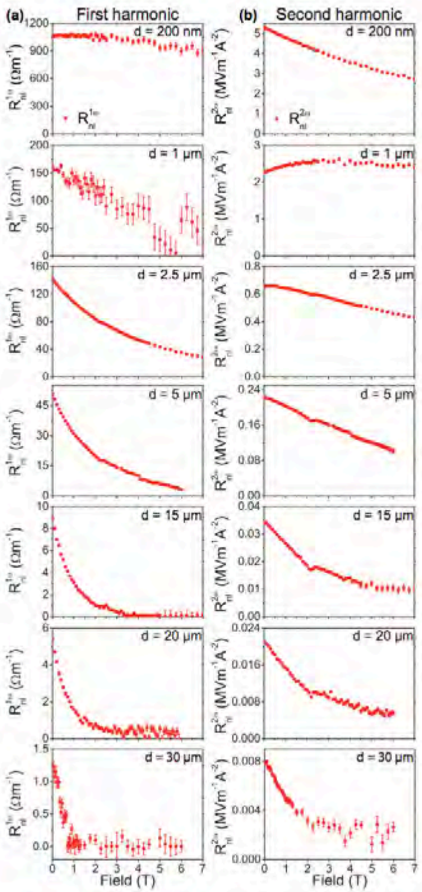

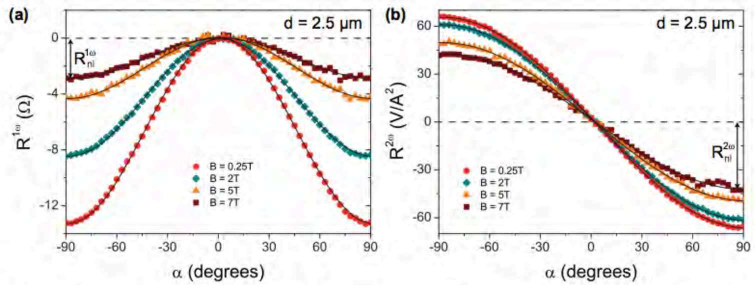

FIG. 2. Nonlocal signal as a function of angle α, for an injector-detector separation distance $d = 2.5\ \mu$m and for various external magnetic field strengths. (a) First-harmonic signal. The solid lines are $\sin^2 \alpha$ fits through the data. (b) Second-harmonic signal. The solid lines are $\sin \alpha$ fits through the data. The decrease in signal amplitude for increasing magnetic field strength is clearly visible for both first- and second-harmonic signals. The amplitudes of the nonlocal signals, $R_{nl}^{1\omega}$ and $R_{nl}^{2\omega}$, are indicated in (a) and (b), respectively, for $B = 7$ T. These measurements were performed using $I_{rms} = 110\ \mu$A at a lock-in frequency of $f = 10.447$ Hz.

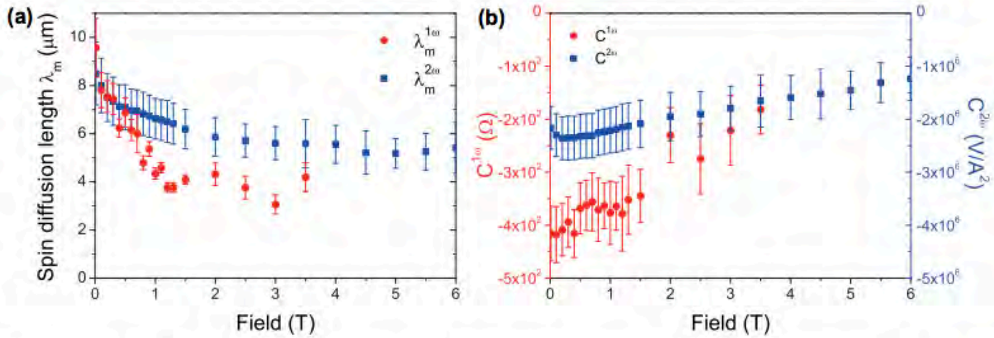

FIG. 5. (a) Magnon spin diffusion length λ_m as a function of external magnetic field, extracted from a fit of Eq. (1) to the distance dependence of the first-harmonic (red circles) and second-harmonic (blue squares) signals. (b) Prefactor C as a function of external magnetic field, extracted from the first (red circles, left axis) and second (blue squares, right axis) harmonic signals.

Experiments involving YIG

PRL 116, 016603 (2016) PHYSICAL REVIEW LETTERS week ending 8 JANUARY 2016

Hanle Magnetoresistance in Thin Metal Films with Strong Spin-Orbit Coupling

Saül Vélez,[1,*] Vitaly N. Golovach,[2,3,4] Amilcar Bedoya-Pinto,[1] Miren Isasa,[1] Edurne Sagasta,[1] Mikel Abadia,[2,3] Celia Rogero,[2,3] Luis E. Hueso,[1,4] F. Sebastian Bergeret,[2,3] and Fèlix Casanova[1,4,†]

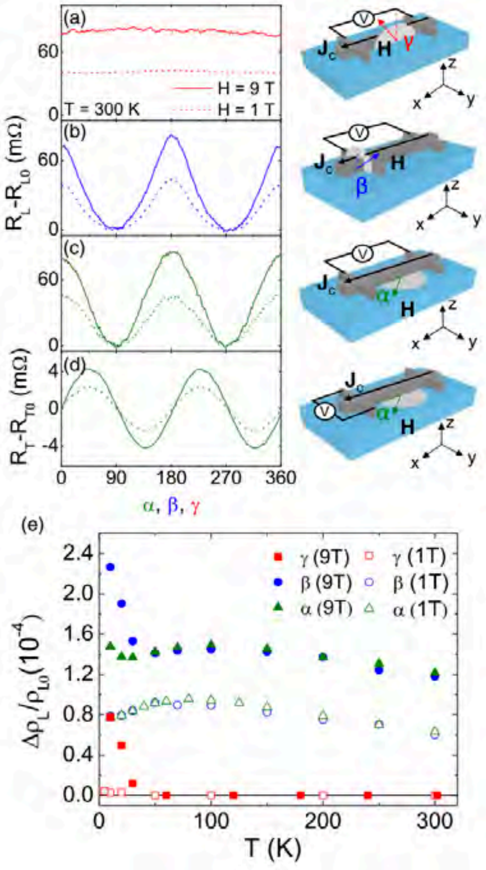

RAPID COMMUNICATIONS

PHYSICAL REVIEW B 91, 220410(R) (2015)

Spin transport in antiferromagnetic insulators mediated by magnetic correlations

Hailong Wang, Chunhui Du, P. Chris Hammel,* and Fengyuan Yang[†]
Department of Physics, The Ohio State University, Columbus, Ohio 43210, USA

(Received 8 February 2015; published 30 June 2015)

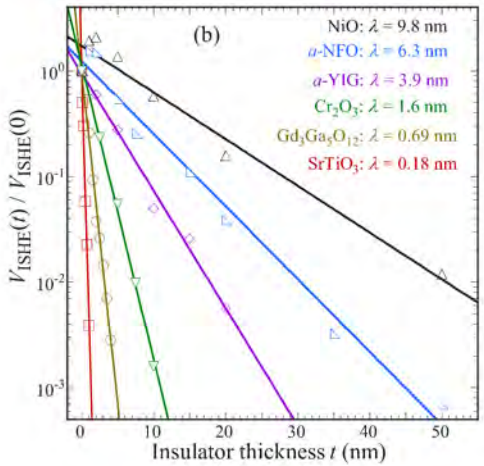

Layer	Magnetism	T_b(K)	λ(nm)	α
epi-YIG	Ferrimagnet			$(8.1 \pm 0.6) \times 10^{-4}$
$SrTiO_3$	Diamagnet		0.18 ± 0.01	$(8.6 \pm 1.0) \times 10^{-4}$
$Gd_3Ga_5O_{12}$	Paramagnet		0.69 ± 0.02	$(11 \pm 1) \times 10^{-4}$
Cr_2O_3	Antiferromagnet	20	1.6 ± 0.1	$(12 \pm 1) \times 10^{-4}$
a-YIG	Antiferromagnet	45	3.9 ± 0.2	$(14 \pm 1) \times 10^{-4}$
a-NFO	Antiferromagnet	70	6.3 ± 0.3	$(17 \pm 2) \times 10^{-4}$
NiO	Antiferromagnet	330	9.8 ± 0.8	$(26 \pm 3) \times 10^{-4}$

Nb/YIG bilayer

Nb/YIG bilayer

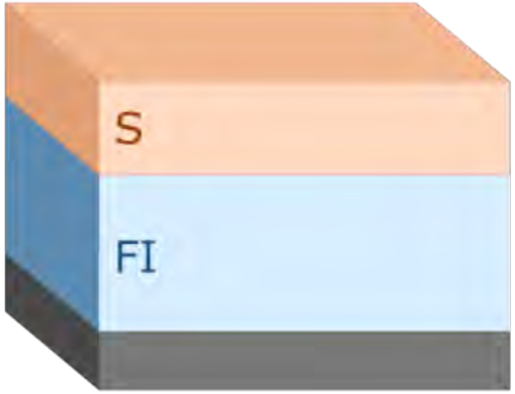

Superconductor: Nb

10-50 nm, magnetron sputtered

Bulk T_c = 9.2 K

YIG

30-60 nm, Pulsed Laser Deposition

GGG ($Gd_3Ga_5O_{12}$) substrate 111 or 110 oriented

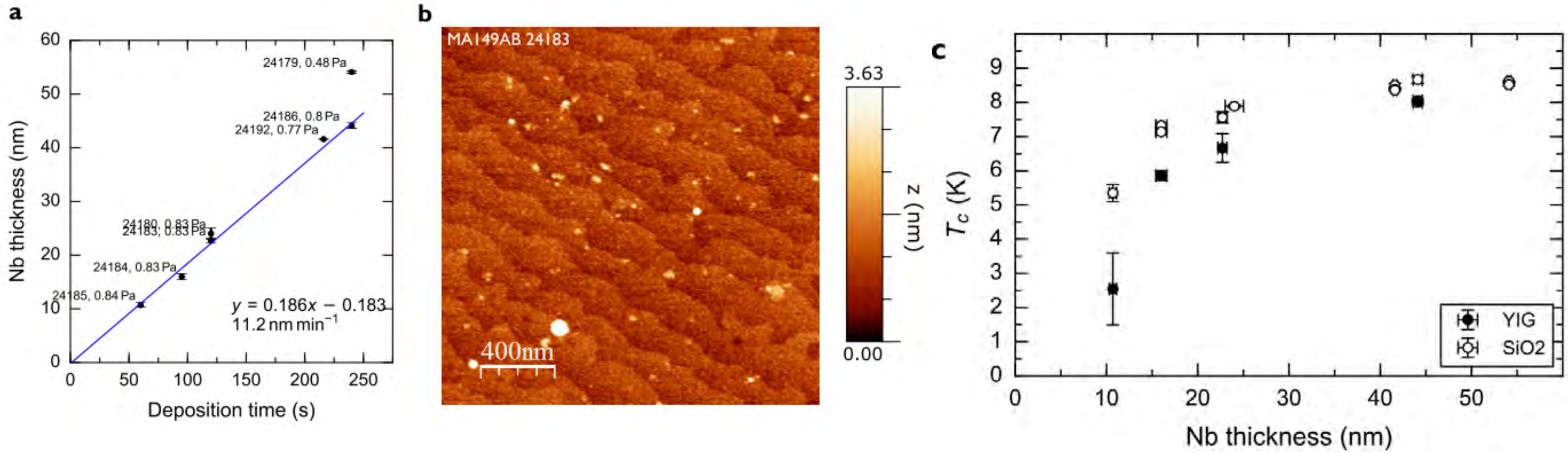

Spin pumping into a superconductor

Ferromagnetic resonance (FMR)

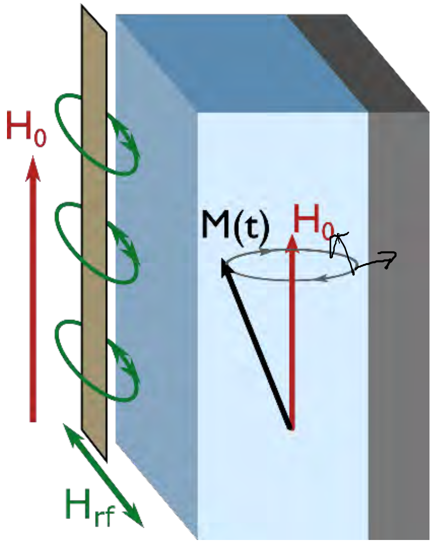

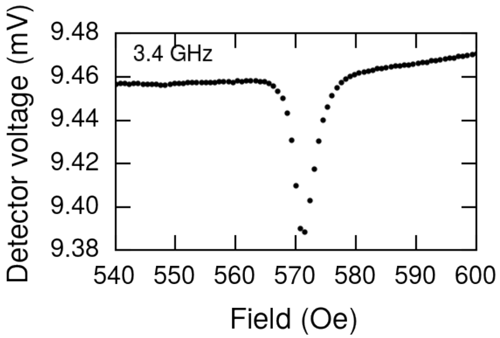

$$f = \gamma\sqrt{H_{res}(H_{res} + 4\pi M)}$$

$$\Delta H(f) = \Delta H_0 + \frac{2\alpha}{\gamma} f$$

Spin pumping

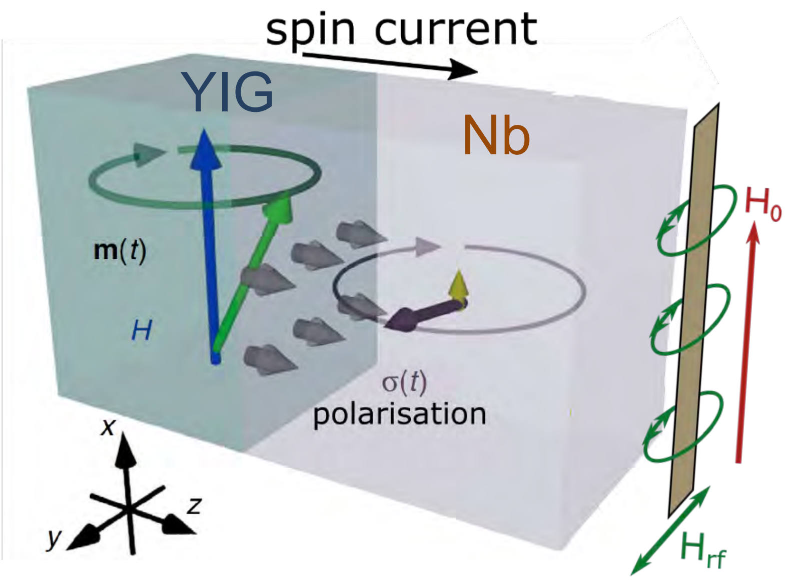

[2]

$$j_s \hat{\boldsymbol{\sigma}} \sim g_r^{\uparrow\downarrow} \frac{1}{M_s^2}\left[\boldsymbol{M}(t)\times\frac{d\boldsymbol{M}(t)}{dt}\right] \text{ [1]}$$

[1] Z. Qiu *et al.* Appl. Phys. Lett. **103**, (2013).

[2] D. Wei *et al.*, Nat Commun **5**, 3768 (2014).

Spin pumping into a superconductor

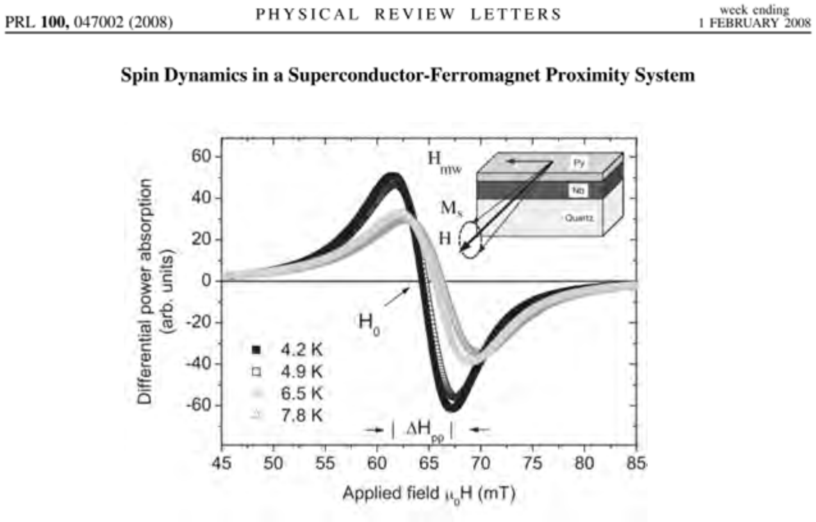

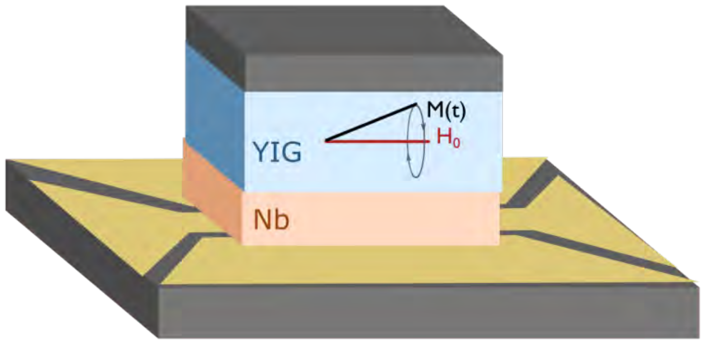

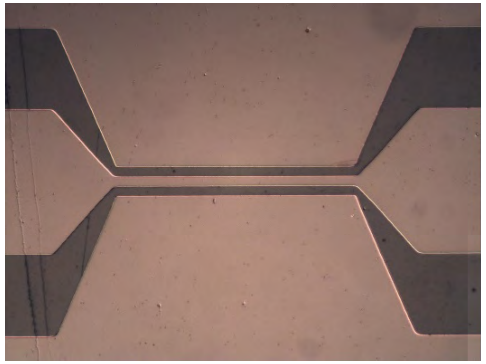

- Permalloy/Nb (metallic FM)
- Cavity FMR (fixed frequency)

- YIG/Nb
- Waveguide FMR

C. Bell, S. Milikisyants, M. Huber, and J. Aarts, Phys. Rev. Lett. **100**, 1 (2008).

Bare YIG: Room temperature FMR

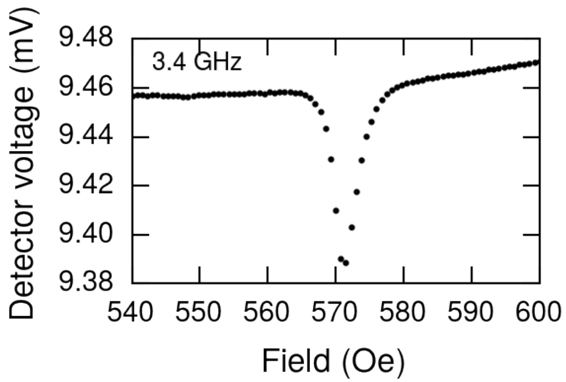

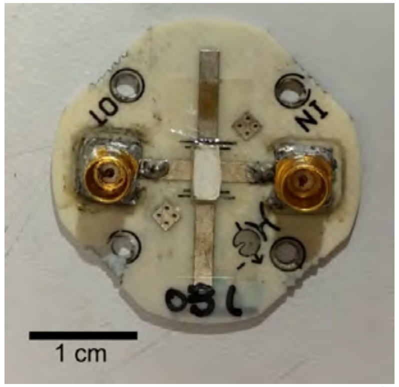

Kittel relation for **in-plane FMR**

$$f = \gamma\sqrt{H_{res}(H_{res} + 4\pi M)}$$

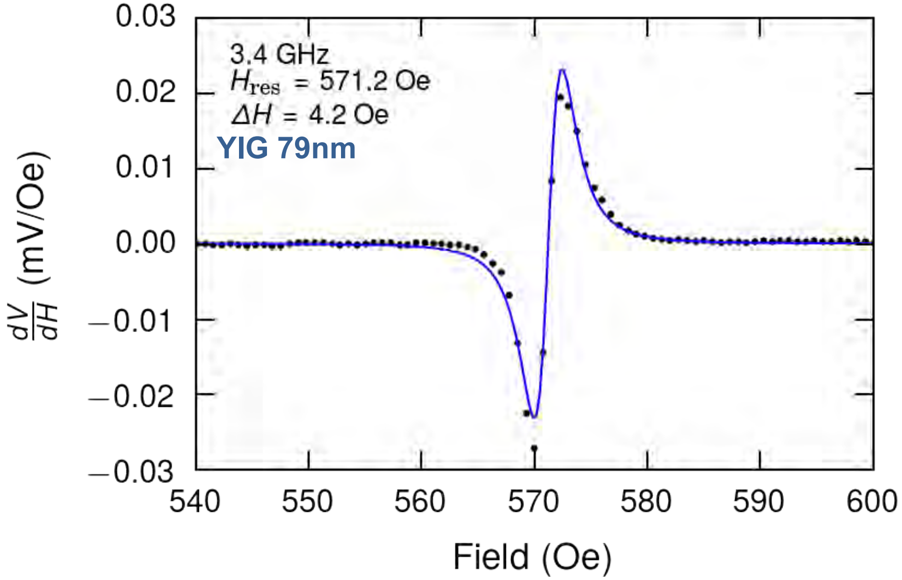

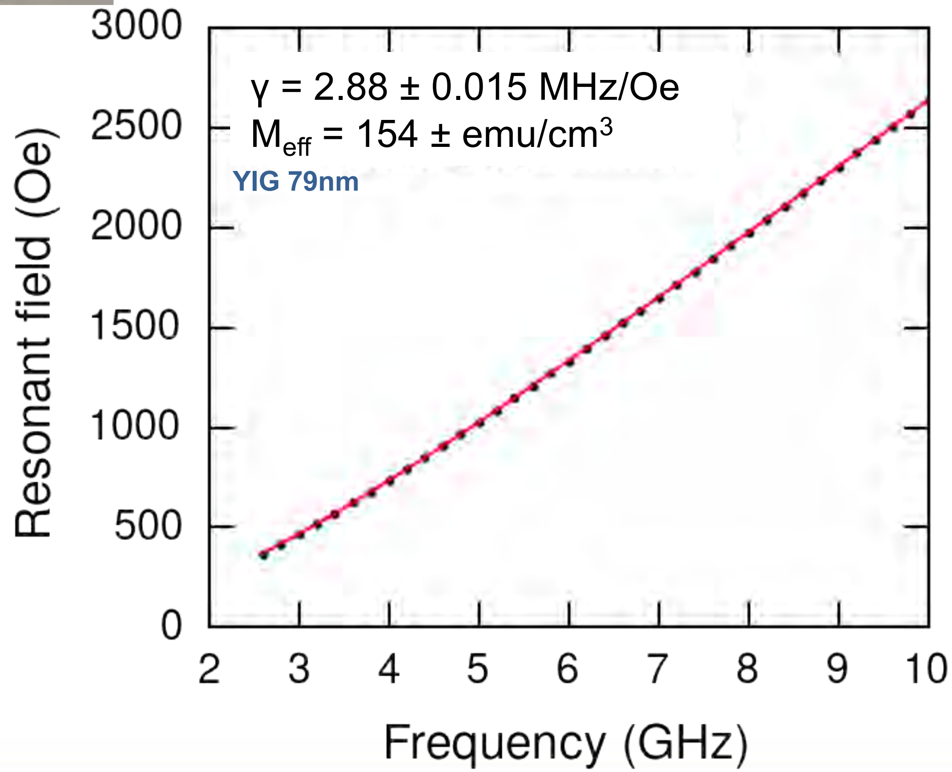

FMR with Nb/YIG – room temperature

Increased damping → Nb is acting as a **spin sink** from the YIG

$$\Delta H(f) = \Delta H_0 + \frac{2\alpha}{\gamma} f$$

Sample	**Damping 10^{-4}**
YIG 79nm	7.3 ± 0.5
YIG 79nm | Nb 37nm	34 ± 1
Jermain et al [1] (15 nm, sputtered)	9.0 ± 0.2
Tang et al. [2] (100 nm, PLD)	~1.0
Hauser et al. [3] (56 nm, PLD)	0.62 ± 0.15

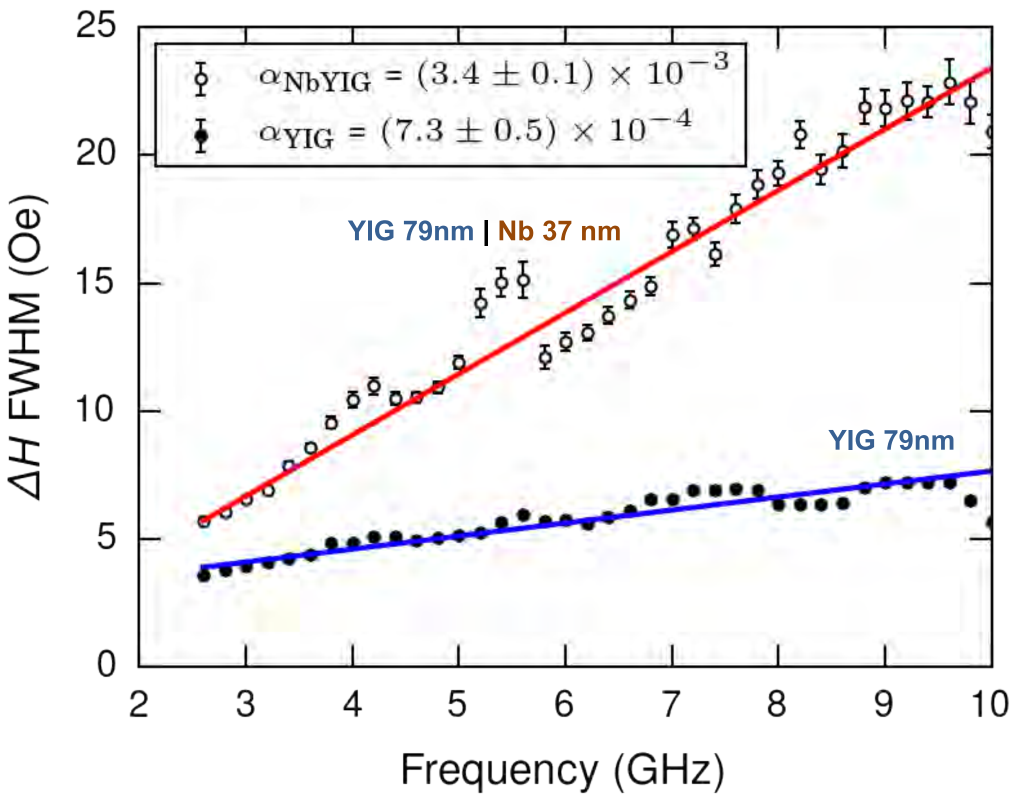

[1] Jermain, C. L. *et al.* (2016).
[2] Tang, C. *et al. Applied Physics Letters* **108,** (2016).
[3] Hauser, C. *et al. Sci. Rep.* 1–13 (2016). doi:10.1038/srep20827

Bare YIG: Low-temperature FMR

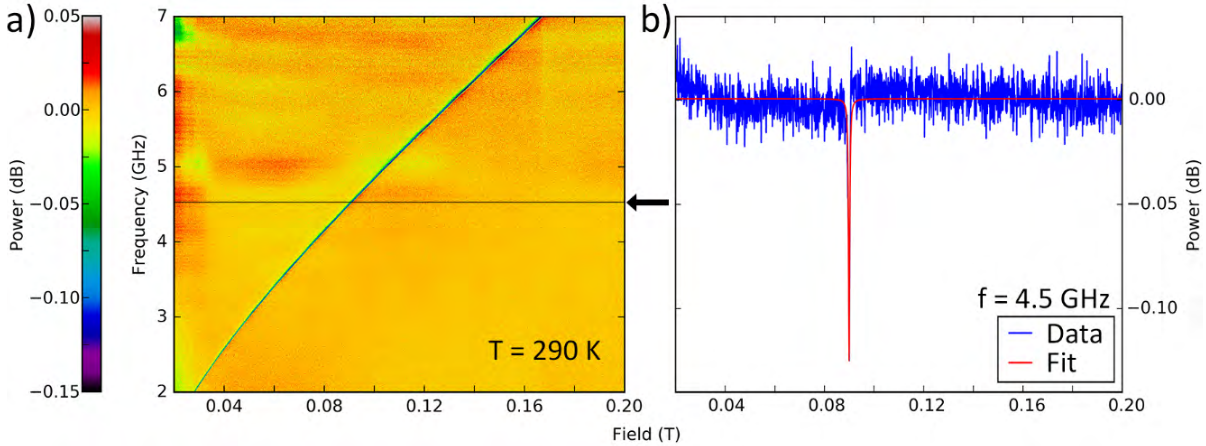

$$f = \gamma\sqrt{H_{res}(H_{res} + 4\pi M)}$$

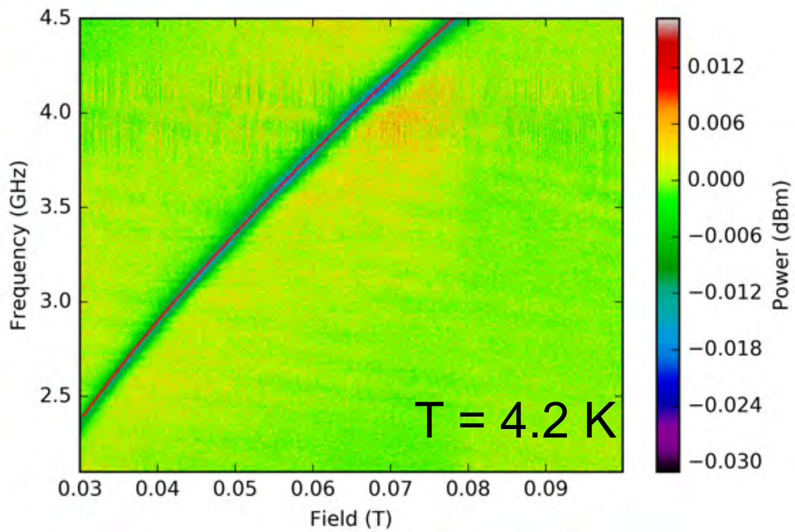

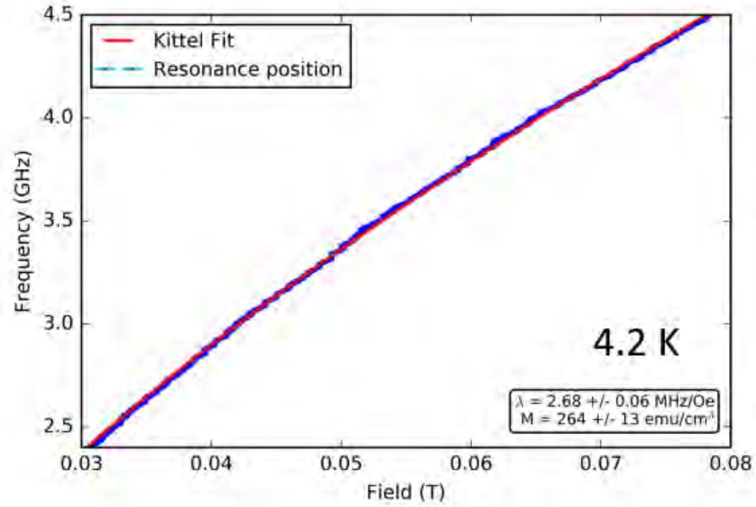

Bare YIG: Temperature-dependent damping

Temperature-dependent damping of bare YIG (VNA measurement)
Filled red markers

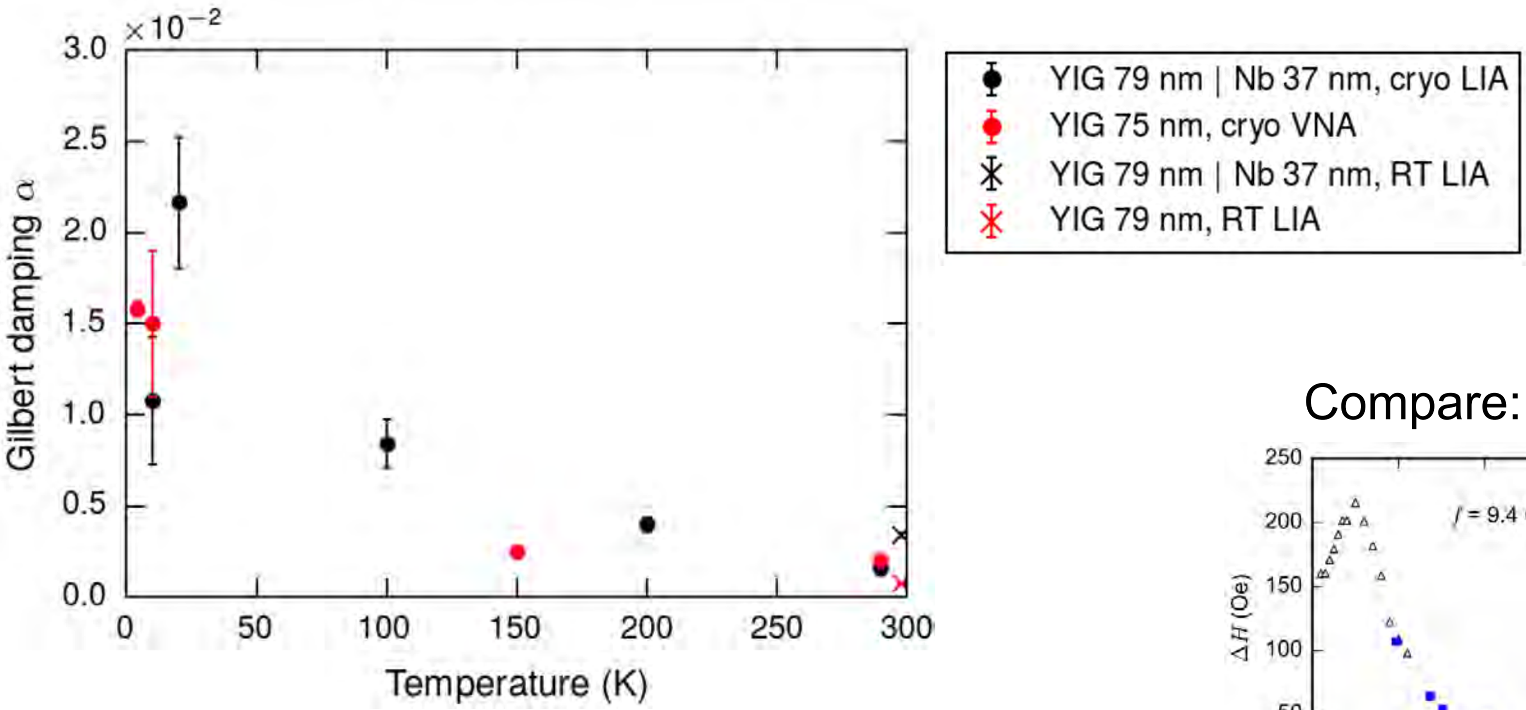

Temp dependence - explanation by Jermain *et al.*
Two magnon scattering
Impurity relaxation

Compare:

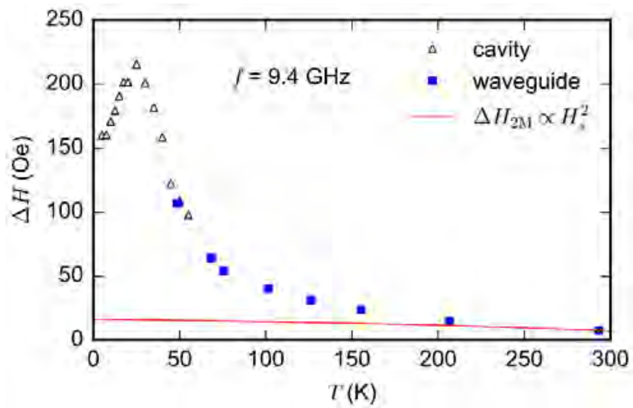

Jermain, C. L. *et al.* Increased low-temperature dampin
yttrium iron garnet thin films. (2016).

Courtesy of
Graham Kimbell

Bare YIG: Effective magnetisation

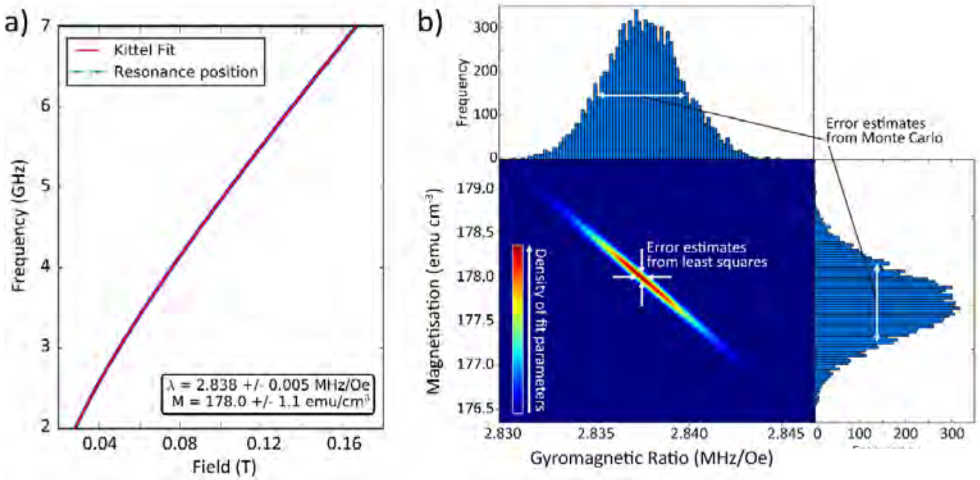

$$f = \gamma\sqrt{H_{res}(H_{res} + 4\pi M)}$$

Note: out-of-plane FMR has different Kittel relation

$$f = \gamma(H_{res} - 4\pi M)$$

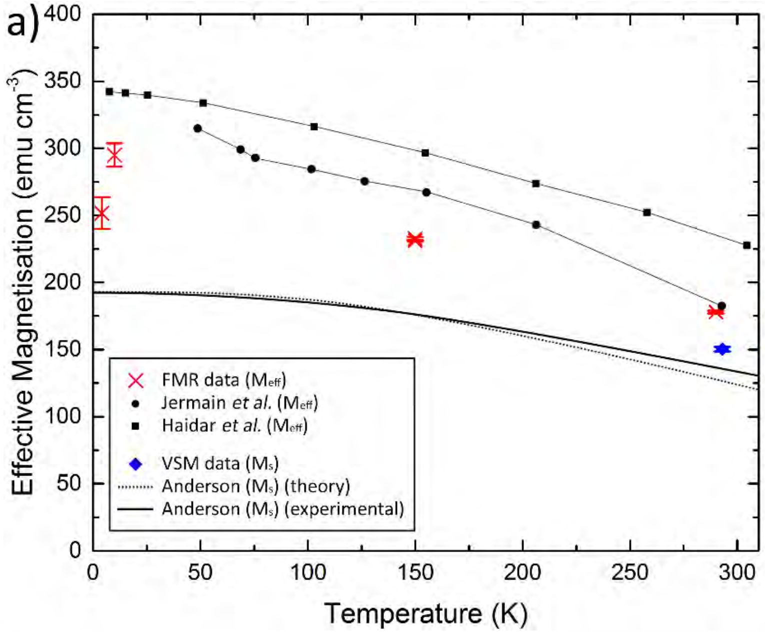

Anisotropy higher than that expected from shape

'Deformation blockage'

H_u = (-350 ± 20) Oe

Jermain, C. L. *et al.* (2016).
Haidar, M. *et al. J. Appl. Phys.* **117,** 115–119 (2015).
Anderson, E. E. *Phys. Rev.* **134,** A1581--A1585 (1964).

Manuilov, S. A. & Grishin, A. M. *J. Appl. Phys.* **106,** 123917 (2009).
Manuilov, S. A. & Grishin, A. M. *J. Appl. Phys.* **108,** (2010).

FMR Nb/YIG – 290 K to 10 K

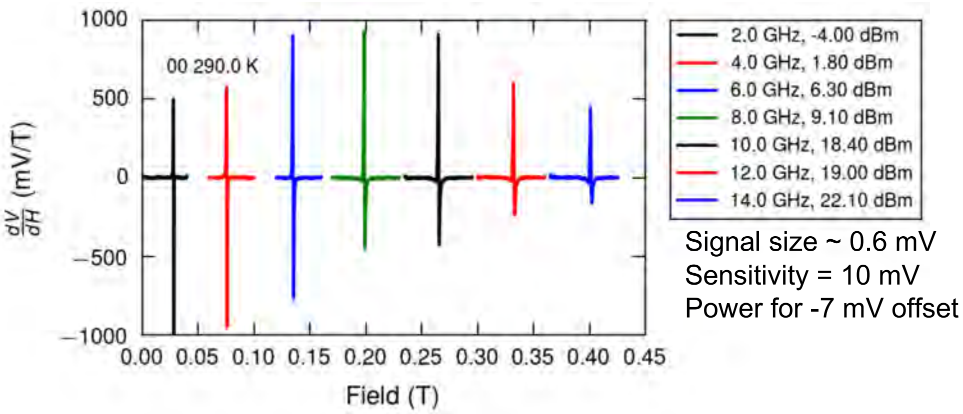

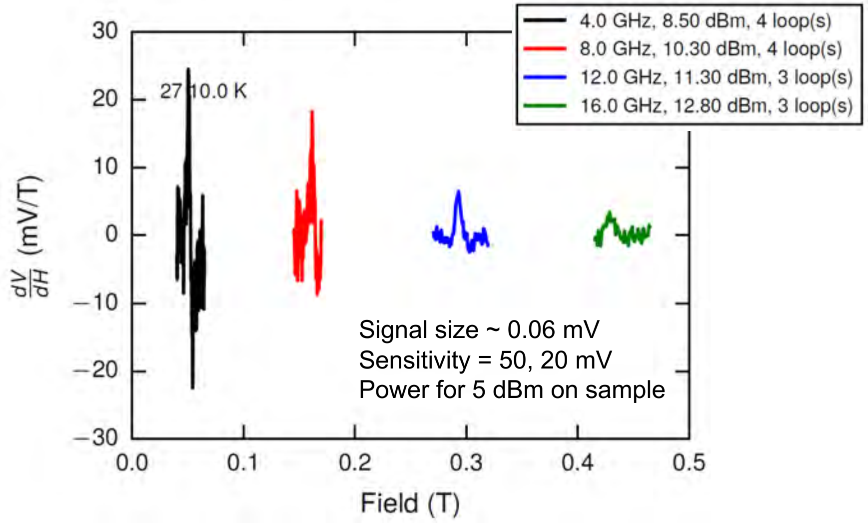

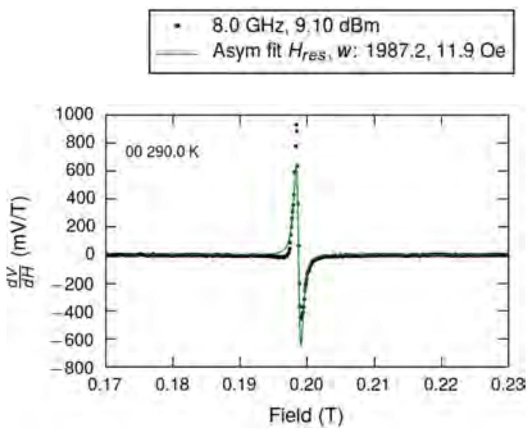

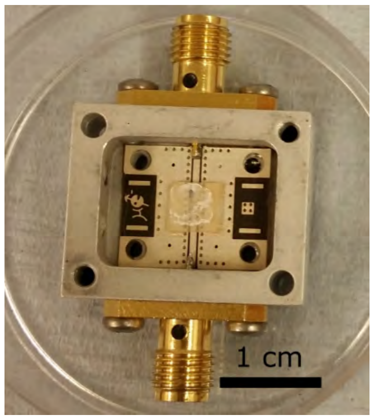

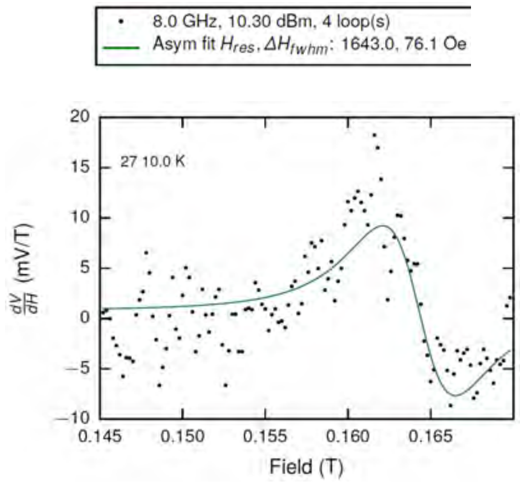

FMR Nb/YIG – below Tc: field modulation

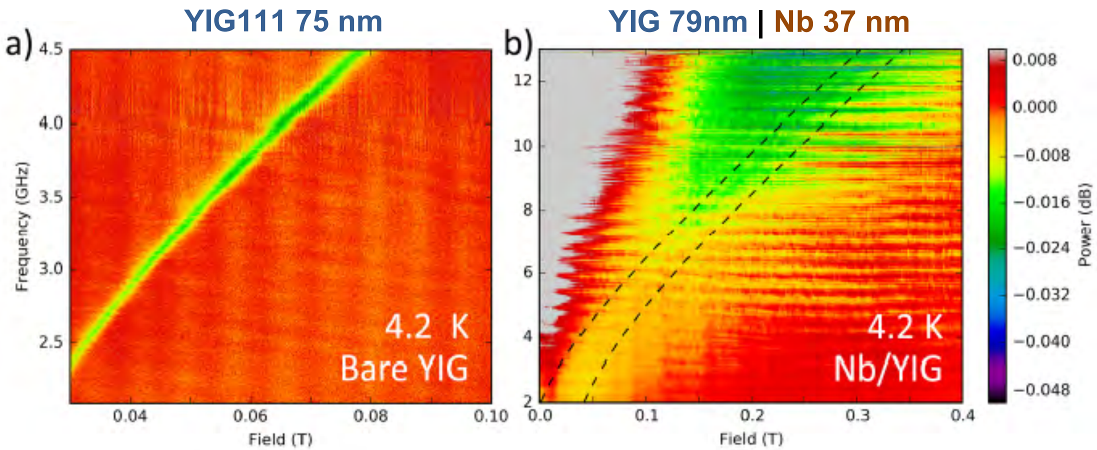

FMR signal weak compared to box background.

Due to the superconducting transition 7.7K

Increased sensitivity by lock-in onto modulated H_0 field and preamplification. Directly obtain signal derivative down to 4.2 K.

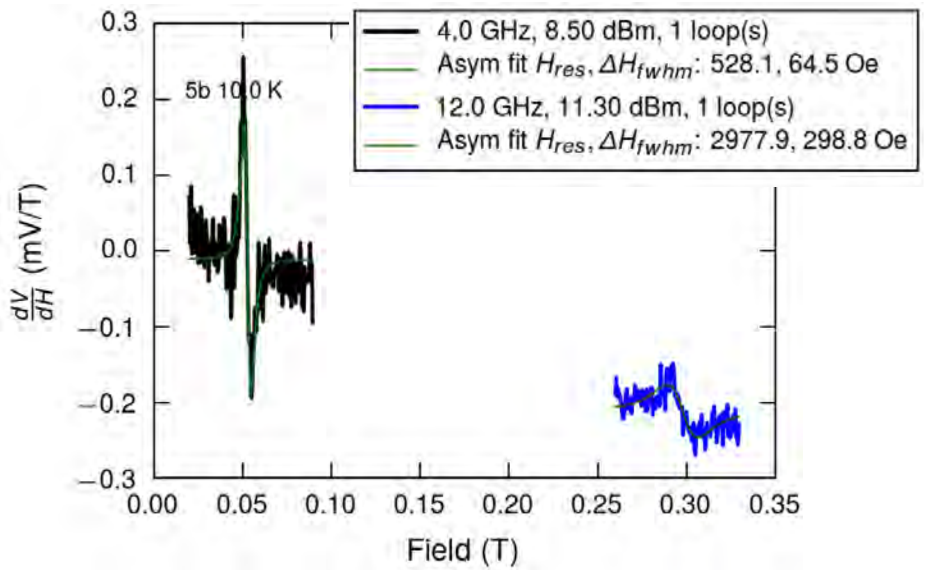

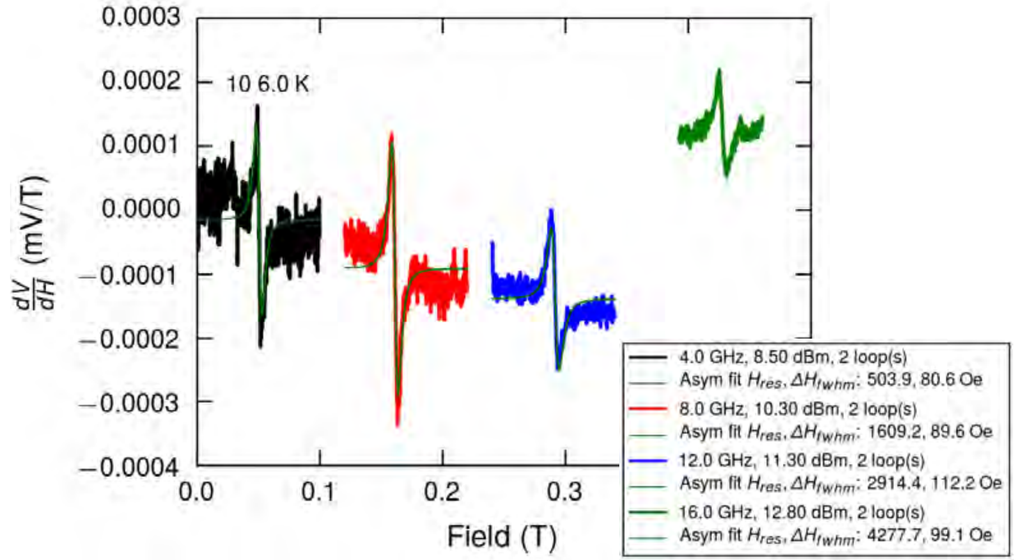

FMR Nb/YIG – Damping

YIG 79nm | Nb 37 nm

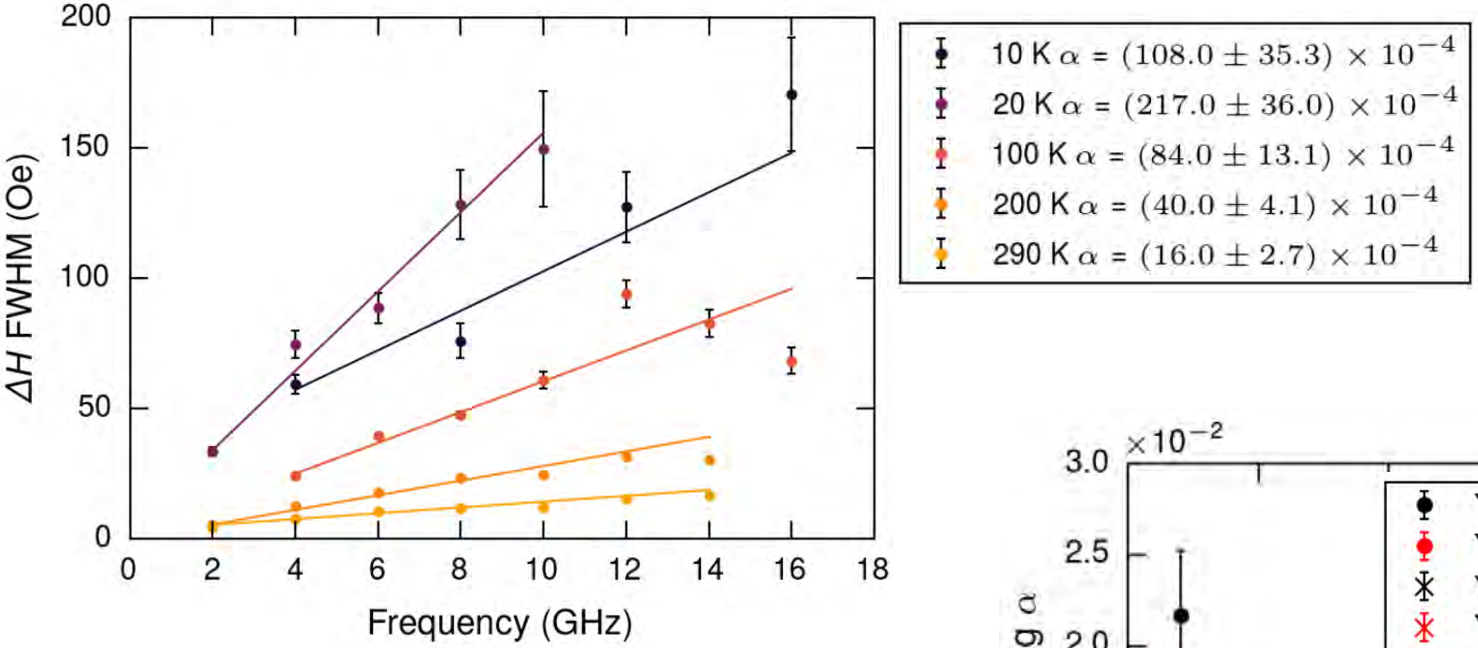

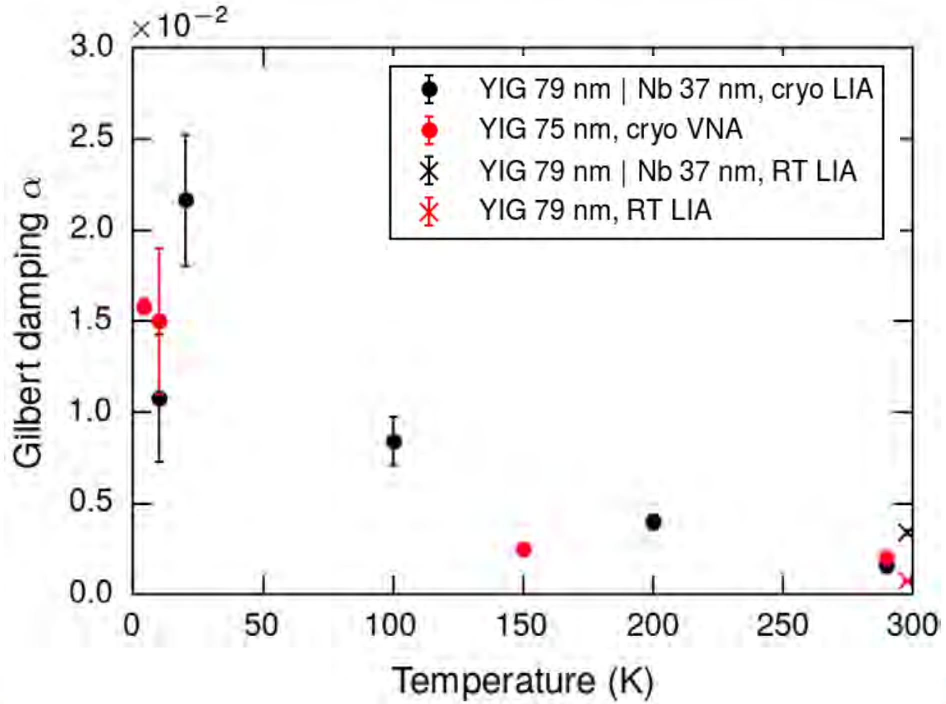

Bi/YIG and Bi-doped Cu/YIG

Bi/YIG and Bi-doped Cu/YIG

- Giant SHE have also been predicted in metals doped with impurities.
- SHA of ~ − 0.24 has been measured [1] in Bi-Cu alloys with ~ 0.5% impurities.
- Compare to Pt which SHA ~ 0.076
- Possibility of having Bi-doped Cu films with a Bi ~ 10% without evidences of segregation or clustering formation

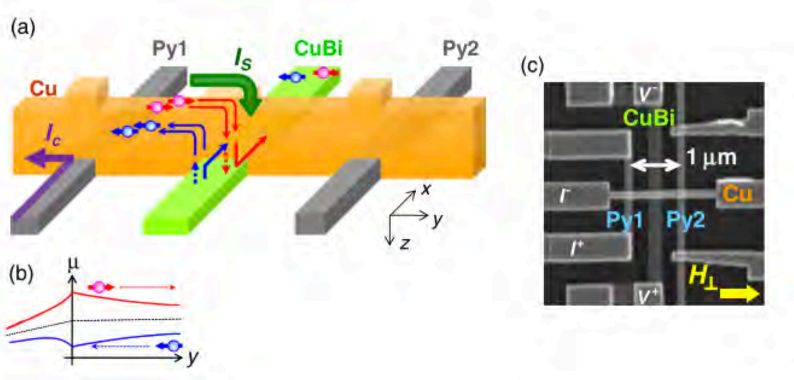

PRL 109, 156602 (2012) PHYSICAL REVIEW LETTERS week ending 12 OCTOBER 2012

Giant Spin Hall Effect Induced by Skew Scattering from Bismuth Impurities inside Thin Film CuBi Alloys

Y. Niimi,[1,*] Y. Kawanishi,[1] D. H. Wei,[1] C. Deranlot,[2] H. X. Yang,[3] M. Chshiev,[3] T. Valet,[4] A. Fert,[2] and Y. Otani[1,5]

Bi/YIG and Bi-doped Cu/YIG

- Giant SHE have also been predicted in metals doped with impurities.
- SHA of ~ − 0.24 has been measured [1] in CuBi alloys with a ~ 0.5% impurities.
- Compare to Pt which SHA ~ 0.076
- Possibility of having Bi-doped Cu films with a Bi ~ 10% without evidences of segregation or clustering formation

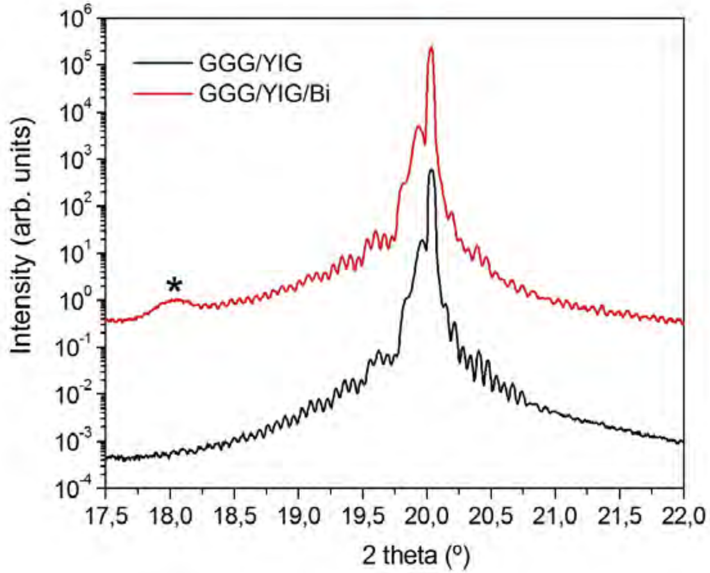

YIG 120nm | Bi 30 nm

-1 1 0 4 Bi

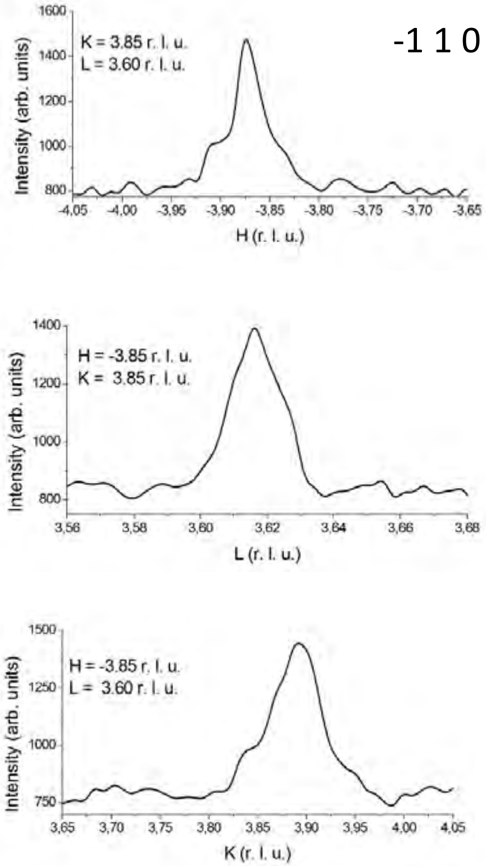

With E. Garcia-Michel, M. Plaza, P. Segovia, UAM Madrid

[1] Y. Niimi, *et al.*, Phys. Rev. Lett. **109**, 156602 (2012).

Band structure Bi/YIG from ARPES @Elettra

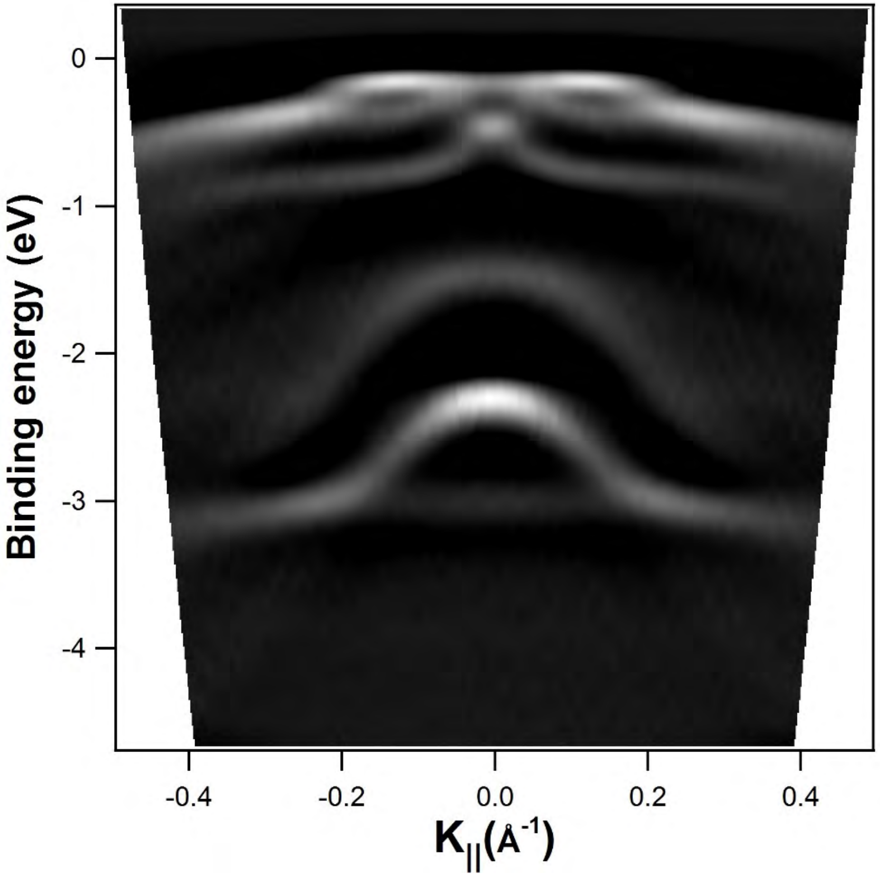

35 nm Bi on YIG 111

Electronic band structure of the Bi film along surface ΓM direction.

The BE origin corresponds to the Fermi level.

In very good agreement with results for single-crystalline Bi(111).

Some bands near the Fermi level correspond to Bi(111) surface states.

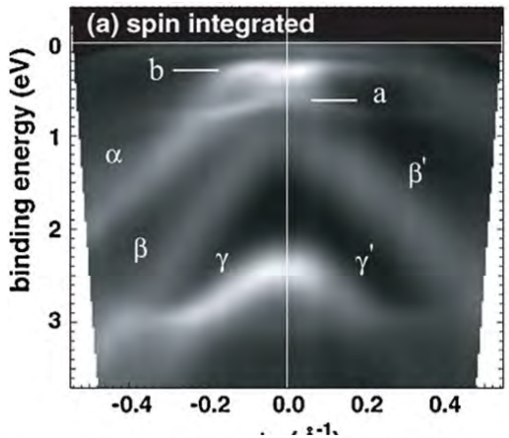

PRL 105, 076804 (2010) PHYSICAL REVIEW LETTERS week ending 13 AUGUST 2010

Strong Rashba-Type Spin Polarization of the Photocurrent from Bulk Continuum States: Experiment and Theory for Bi(111)

A. Kimura,[1,*] E. E. Krasovskii,[2,3,4] R. Nishimura,[1] K. Miyamoto,[5] T. Kadono,[1] K. Kanomaru,[1] E. V. Chulkov,[2,3,6] G. Bihlmayer,[7] K. Shimada,[5] H. Namatame,[5] and M. Taniguchi[1,5]

Band structure Bi/YIG from ARPES @Elettra

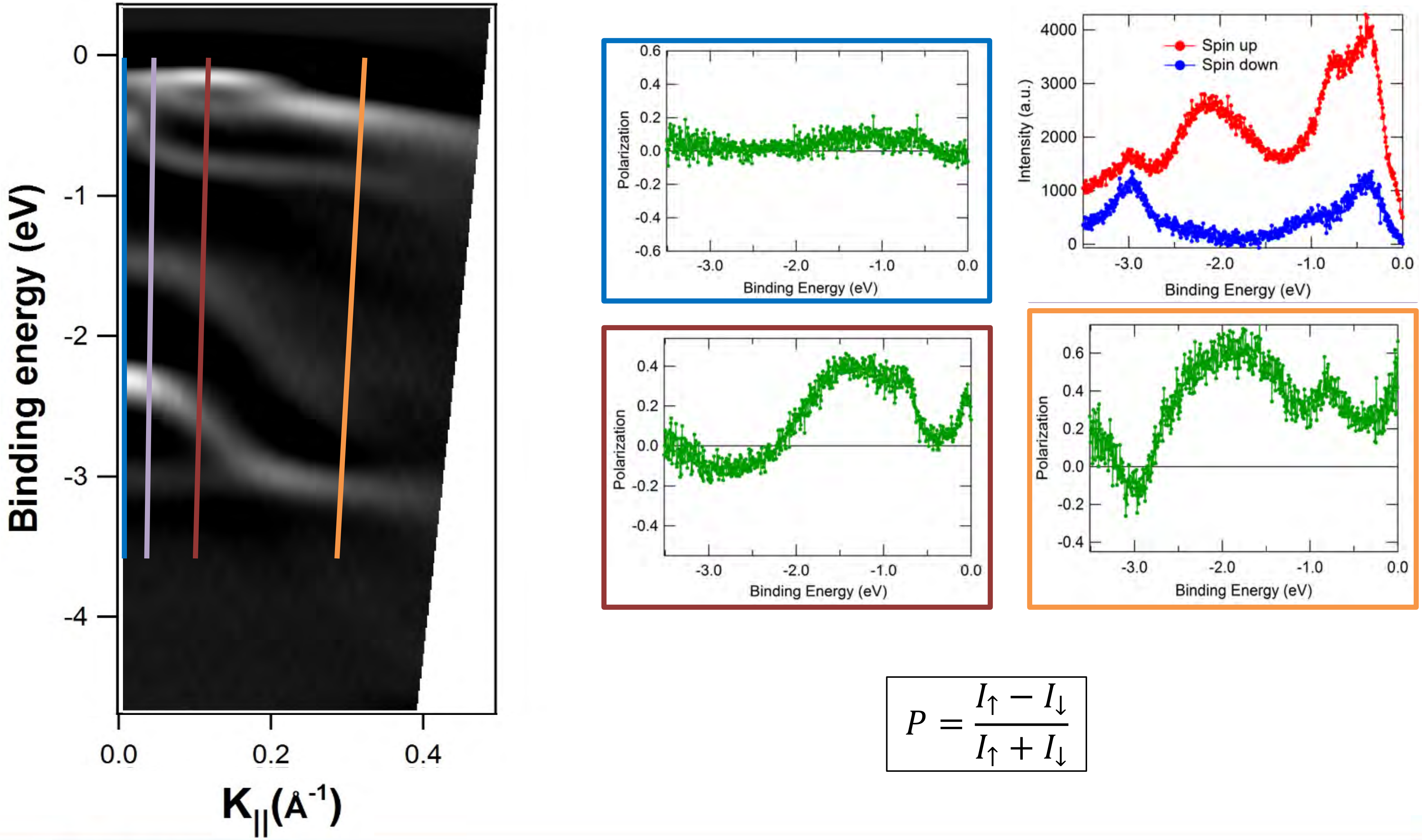

$$P = \frac{I_{\uparrow} - I_{\downarrow}}{I_{\uparrow} + I_{\downarrow}}$$

Band structure Bi/YIG from ARPES @Elettra

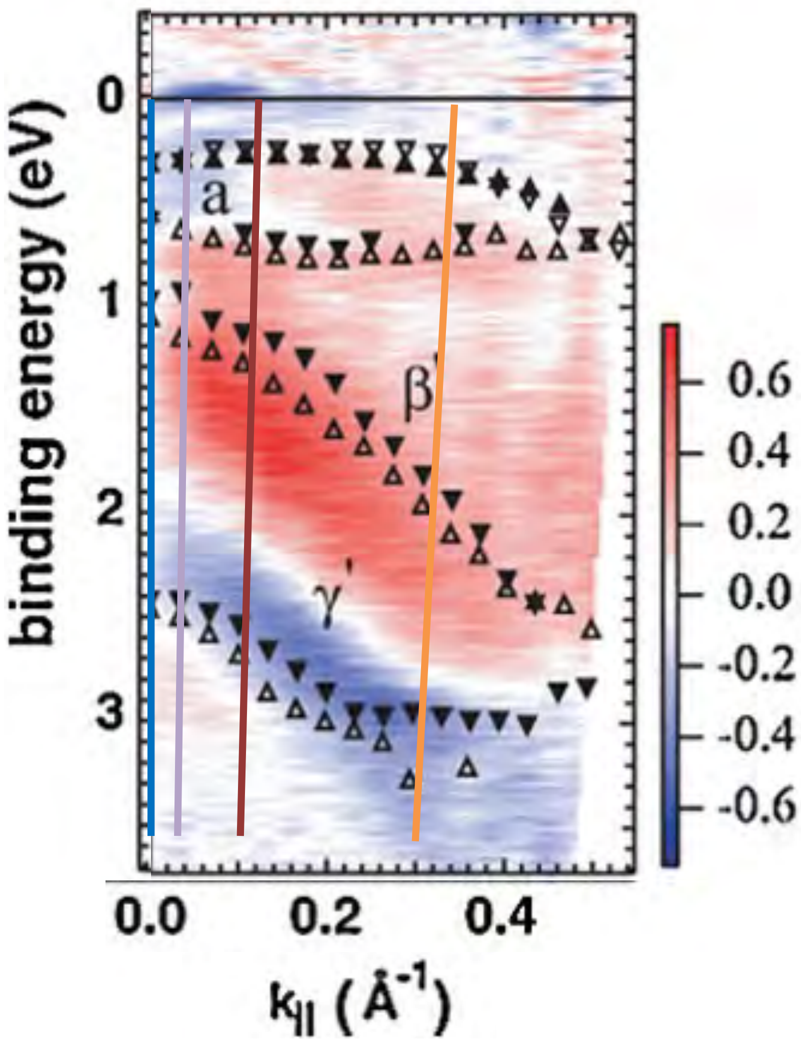

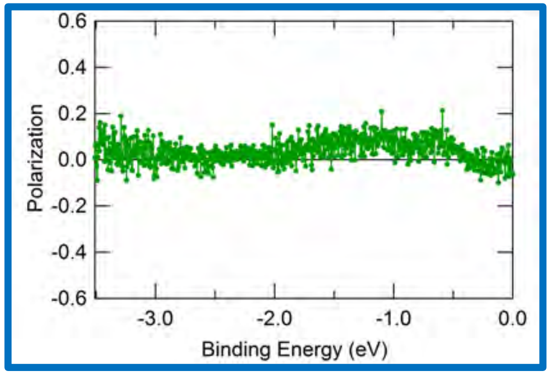

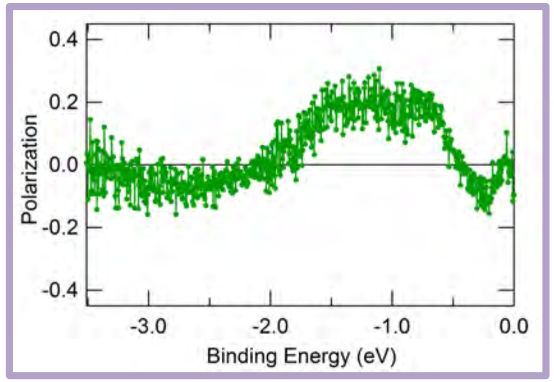

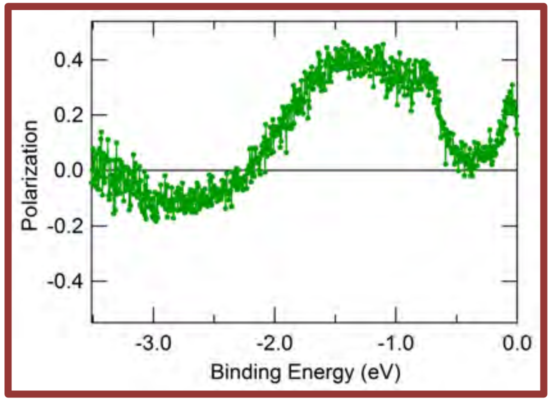

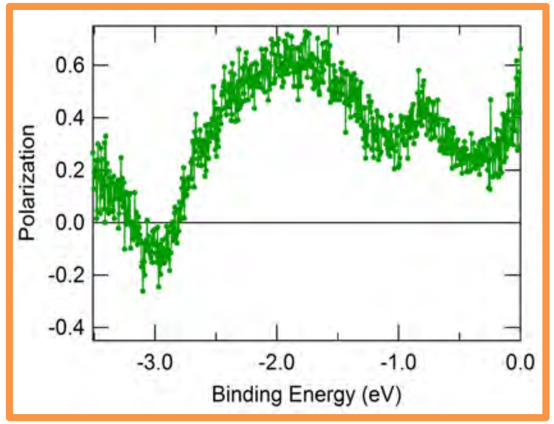

PRL **105,** 076804 (2010) PHYSICAL REVIEW LETTERS week ending 13 AUGUST 2010

Strong Rashba-Type Spin Polarization of the Photocurrent from Bulk Continuum States: Experiment and Theory for Bi(111)

A. Kimura,[1,*] E. E. Krasovskii,[2,3,4] R. Nishimura,[1] K. Miyamoto,[5] T. Kadono,[1] K. Kanomaru,[1] E. V. Chulkov,[2,3,6] G. Bihlmayer,[7] K. Shimada,[5] H. Namatame,[5] and M. Taniguchi[1,5]

Bi-doped Cu/YIG

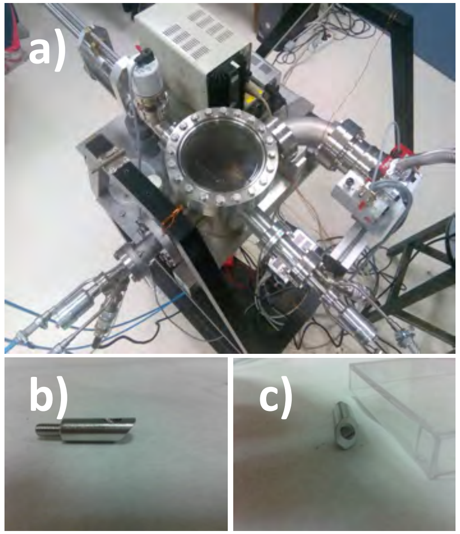

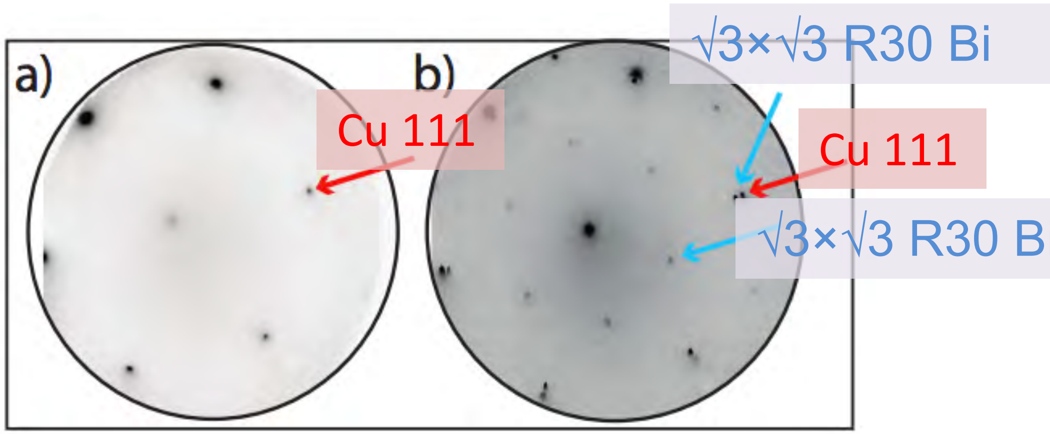

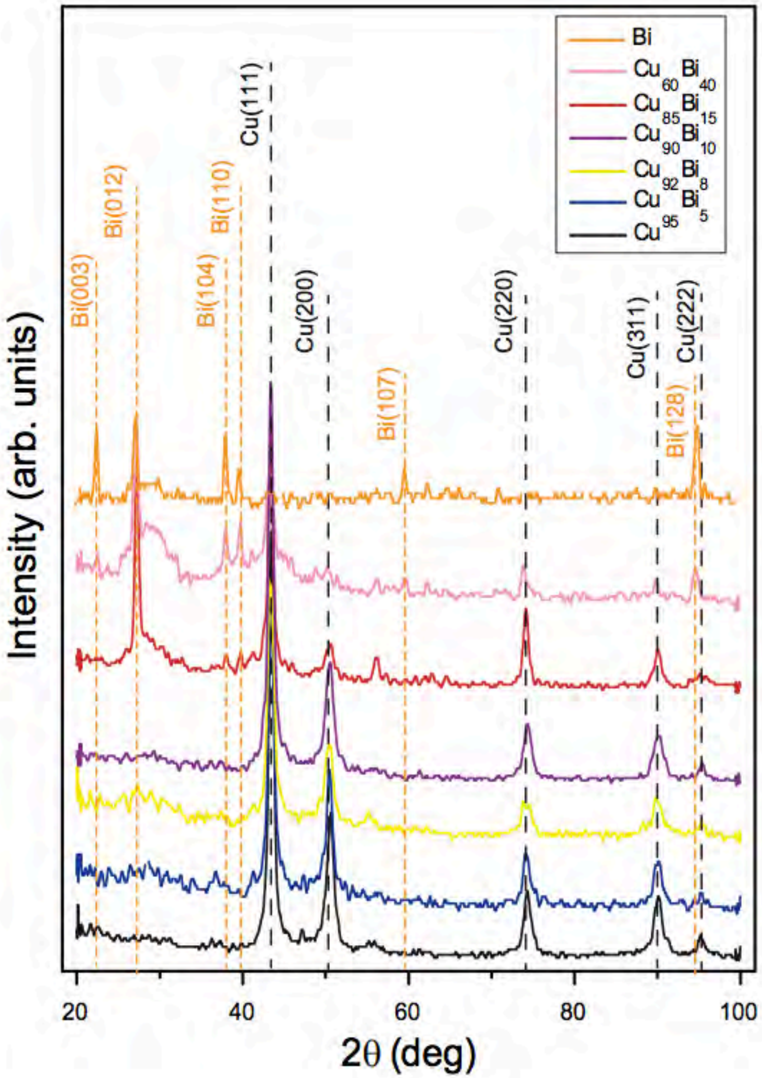

Bi-doped Cu/YIG

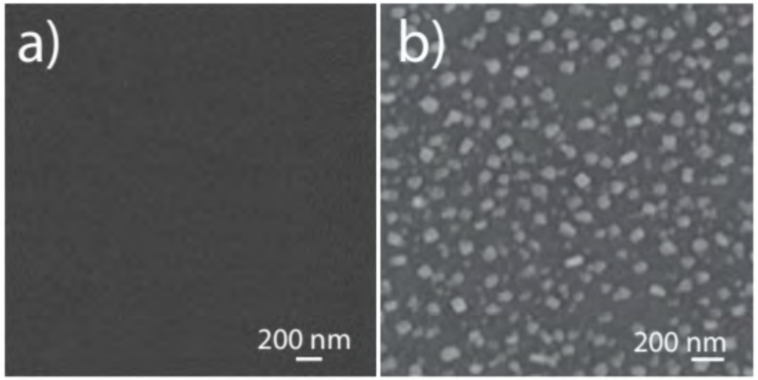

Bi_5Cu_{95} $Bi_{40}Cu_{60}$

$Bi_{25}Cu_{75}$ Bi_5Cu_{95}

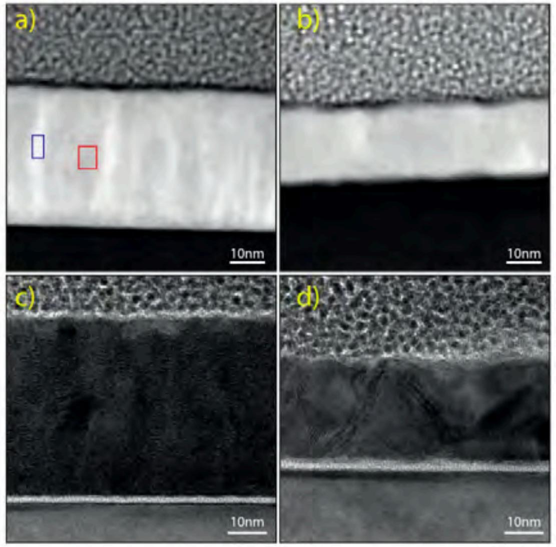

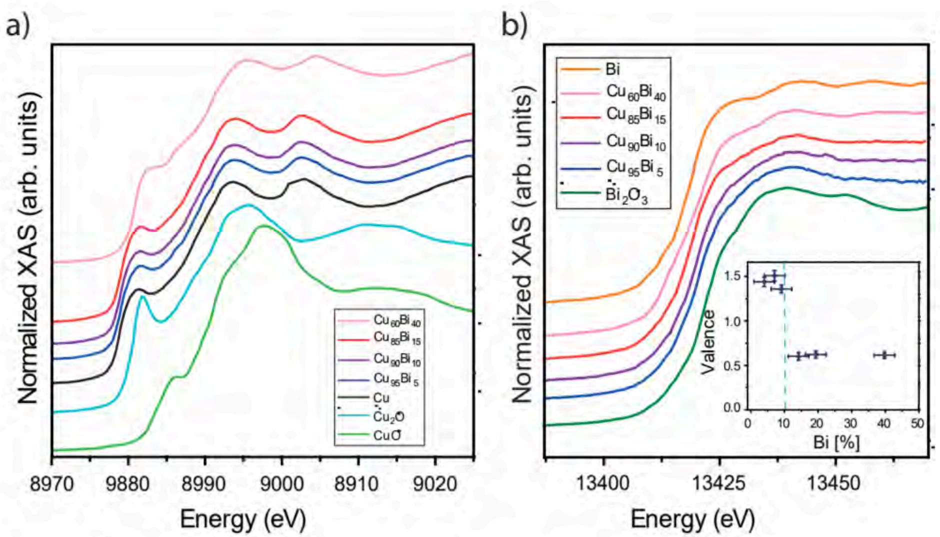

Bi-doped Cu/YIG FMR RT

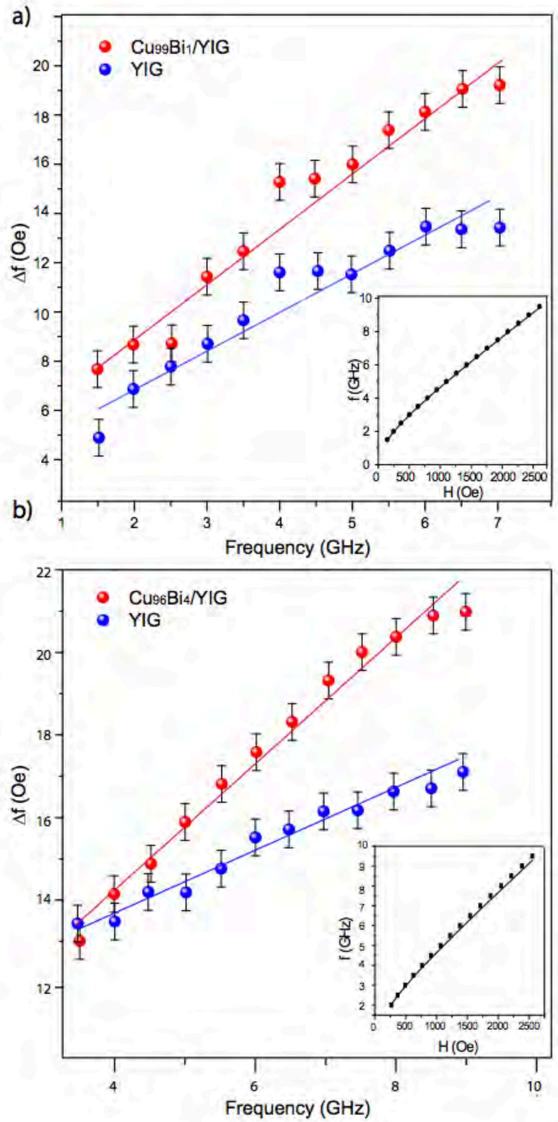

$$\Delta H_{FMR} = \Delta H_0 + \frac{2 \propto}{\sqrt{3}|\gamma|}\frac{w}{2\pi}$$

YIG: $\propto = 3.7\text{x}10^{-3}$ — 50% increase at RT

$Cu_{99}Bi_1$/YIG: $\propto = 5.4\text{x}10^{-3}$

$$\Delta H_{FMR} = \Delta H_0 + \frac{2 \propto}{\sqrt{3}|\gamma|}\frac{w}{2\pi}$$

YIG: $\propto = 1.7\text{x}10^{-3}$ — 100% increase at RT

$Cu_{96}Bi_4$/YIG: $\propto = 3.7\text{x}10^{-3}$

Conclusions and further work

- High quality YIG thin film growth, Nb/YIG bilayer deposition.

- Room temp. FMR
  - YIG damping: 7 *10^{-4} for ~ 80 nm
  - Nb/YIG damping: increases by 5x
- FMR examining additional magnetic phenomena in YIG at low temperatures
  - Temperature dependent magnetisation and damping
  - Connection to growth & RT properties
- Spin-pumping in Nb/YIG being extended to below Nb T_c (7.7 K) using field modulation and preamplification.

- Bi/YIG and Bi-doped Cu/YIG for spin pumping and SHE
  - $Cu_{90}Bi_{10}$/YIG achievable
  - Low temperature FMR in progress